Mooring Analysis in Offshore Floating Labs: Case Study on a 15MW Wind Platform

Chenyu Zhao [a], Jiaxin Chen [a,*], Lars Johanning [a]

[a] School of Engineering, Computing and Mathematics, University of Plymouth

Plymouth, Devon, United Kingdom. PL4 8AA.

[*] Corresponding author: Jiaxin.chen@plymouth.ac.uk

Abstract

As floating offshore wind turbines (FOWTs) expand into deeper and more complex marine environments, validating mooring system performance under real-world conditions becomes critical. This study investigates whether a scaled offshore floating laboratory (OffLab), named ACTOR, can serve as an effective and conservative testbed for mooring line evaluation. ACTOR is a 1:3 scale conceptual platform based on the UMaine VolturnUS-S 15 MW semi-submersible FOWT design, and is intended for deployment in a nearshore UK site with milder sea conditions. Using site-specific environmental data from two locations—the full-scale deployment zone in the Celtic Sea and a nearshore test location near Plymouth Sound—we perform comparative mooring analyses with OrcaFlex. Extreme load cases are defined using Direct-IFORM environmental contours, and fatigue conditions are derived from long-term wave spectral clustering. Results show that due to shallow water effects and tailored pre-tensioning, the ACTOR platform can replicate or exceed the mooring line tensions and fatigue damage accumulation observed in full-scale systems (mooring line lifespan for ACTOR and FOWT are 63 years to 11.6 year, respectively). The findings demonstrate the potential of ACTOR as a physically accessible, cost-effective platform for accelerated offshore component testing.

Keywords: Offshore Floating Laboratory, Mooring System, Extreme Load Analysis, Fatigue Testing, OrcaFlex

1. Introduction

Wind energy has experienced a remarkable evolution, transitioning from onshore installations to offshore developments, and progressively advancing from nearshore to far-offshore locations. This shift is driven by the stronger and more consistent wind resources found further from coastlines (Tumse et al., 2024). Offshore wind offers several advantages, including access to higher wind speeds and the ability to deploy larger turbines. In 2010,

offshore wind capacity was a modest 3.1 GW, but by 2020, it had expanded to 34.4 GW, reflecting a more rapid growth rate compared to onshore wind (McCoy et al., 2024). At the same time, this expansion of offshore wind energy into deeper waters has introduced significant challenges, particularly concerning the test of mooring systems for floating offshore wind turbines (FOWTs). Yang et al. (2022) gave a comprehensive review of the mooring system design for the FOWTs and pointed out the future research trends would focus on the more complex hybrid configurations and new materials.

However, above new trend may bring more challenges during the mooring line testing process. One primary challenge is achieving accurate scaling in physical models. Testing often involves scaled-down versions of mooring systems in wave basins or flumes. Maintaining geometric, kinematic, and dynamic similarity requires careful adherence to scaling laws, such as Froude scaling for gravitational forces. Some phenomena, like viscous effects, do not scale linearly, leading to discrepancies between model tests and real-world behaviour. This necessitates the use of advanced materials and techniques to mimic the properties of full-scale mooring lines accurate (Hmedi et al., 2023; Matha et al., 2011). Replicating the harsh and variable ocean conditions in a laboratory is another significant hurdle. Mooring lines in operational settings are subjected to complex loading from wind, waves, and currents. Creating a controlled environment that accurately simulates these combined forces is challenging (Timmington & Efthimiou, 2022). The final critical consideration is the fatigue of the mooring line. Accurately replicating these dynamic loads in testing environments is challenging but essential for assessing the long-term performance of mooring systems. However, the fatigue tests are always dry test which cannot fully consider the mooring line corrosion in the sea water(Matha et al., 2011).

This transition also introduces new financial and operational risks, particularly in the context of insurance coverage for floating wind technologies. Insurers assess offshore wind projects based on their technology readiness level (TRL) and historical performance data. Given that dynamic mooring systems, floating substations, and high-voltage export cables remain in the early stages of full-scale deployment, insurance premiums and risk mitigation strategies are critical concerns. Floating wind projects face higher estimated maximum loss (EML) scenarios, particularly due to potential failures in mooring integrity, power transmission systems, and extreme weather exposure. These risks can lead to significant delays and financial losses, making early-stage testing and validation essential for securing cost-effective insurance policies (Clark, 2024).

Offshore laboratories (OffLabs) offer a middle ground between numerical modelling and full-scale deployment, enabling controlled yet realistic testing of floating wind components. Examples include HarshLab 2.0 (Touzon et al., 2020), Blue Accelerator (Carpintero Moreno et al., 2020), and OCG-DATA (Dobson et al., 2024). This study introduces ACTOR, an Offshore Floating Laboratory currently under development in the southwest UK. With the Crown Estate's targeting the development of FOWT projects in the Celtic Sea by 2030 (Estate, 2023),

the demand for such an OffLab has intensified to de-risk essential components and sub-systems before at-sea testing. Based on a 1/3-scale version of the UMaine VolturnUS-S 15MW platform (Allen et al., 2020), ACTOR is designed to evaluate mooring system performance under real sea conditions. Unlike FOWTs, it does not include a wind turbine but is instead tailored for experimental testing of mooring lines, cables, sensors, and structural response in a nearshore environment.

Due to the differences in scale and target deployment areas—deep offshore sites for FOWTs versus nearshore locations for OffLabs—environmental loading differs significantly. However, because mooring systems rely on suspended weight for restoring force, the OffLab moorings may experience higher loads due to shallower water and increased stiffness. This study investigates whether the scaled ACTOR platform, operating in a nearshore environment, can replicate or exceed the mooring loads seen in full-scale offshore platforms. If validated, ACTOR can serve as a conservative yet efficient testbed for accelerated component qualification.

This study presents a comparative mooring analysis between the full-scale 15MW FOWT and the ACTOR platform (Figure 1), using OrcaFlex (Orcina, 2024) simulations to evaluate their respective responses to extreme and fatigue environmental conditions. The ACTOR platform is currently a conceptual design, and no physical deployment has occurred. The primary goal is to assess its effectiveness as a testbed by comparing load magnitudes, frequency of extreme events, and fatigue accumulation to those in full-scale deployment. Key research questions include:

1. Can an OffLab (ACTOR) effectively generate extreme mooring line tensions comparable to those of a full-scale offshore wind platform under different sea condition?
2. Does the ACTOR platform accelerate fatigue damage through pre-tension alteration?
3. What are the key differences in load distribution, frequency of transient extreme events, and fatigue damage accumulation between the OffLab and full-scale platforms?

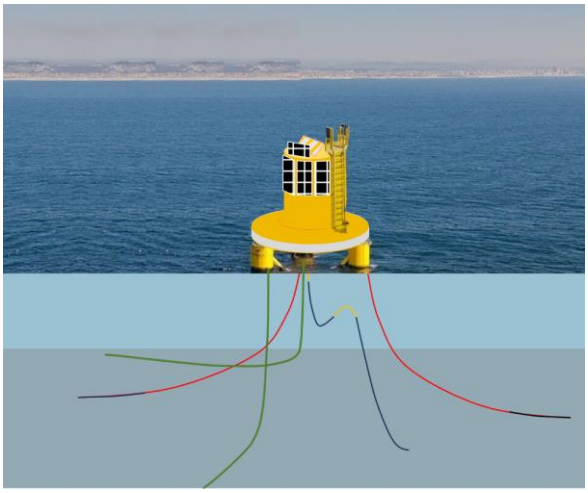

Figure 1 Conceptual illustration of the ACTOR OffLab platform. The topside is inspired by the HarshLab and adapted for visualisation purposes.

The remainder of this paper is structured as follows: Section 2 presents the case study development, detailing the full-scale and ACTOR scaled platforms, mooring configurations, and environmental conditions. Section 3 describes the analytical approach, including extreme load analysis, fatigue assessment, and mooring chain design. Section 4 provides results and discussions, comparing the mooring system performance of the two platforms under various environmental conditions. Finally, Section 5 concludes the study by summarizing key findings, validating the ACTOR platform's effectiveness, and suggesting future research directions.

2. Case study development

To investigate the feasibility of using the scaled OffLab ACTOR for mooring system evaluation, two representative platforms and deployment sites were selected. The full-scale reference platform is the UMaine VolturnUS-S (Allen et al., 2020), a 15 MW floating wind turbine with a three-column semi-submersible hull, designed for deep offshore deployment in the Celtic Sea. The scaled experimental platform (ACTOR) is derived from this reference design with a 1:3 geometric and mass scaling factor. While the ACTOR platform omits the wind turbine and tower components, it preserves the primary structural layout and mooring design principles to allow for focused testing of mooring line response.

The ACTOR platform is intended for nearshore deployment at Smart Sound Plymouth, an area with established monitoring infrastructure and easier access for operations. In contrast, the full-scale platform is hypothetically deployed at a Celtic Sea location aligned with the Crown Estate’s Project Development Areas (PDAs) (Estate, 2023). These two sites differ significantly in environmental conditions, particularly water depth and wave climate. However, shallow water induces increased mooring line stiffness and larger dynamic tension responses. This makes it plausible that ACTOR, despite being in a milder met-ocean environment, could replicate or even amplify the mooring load conditions experienced offshore.

Scenario-Based Environmental Conditions

This Celtic Sea area has characteristic depth of 80 m. The ACTOR platform site is located near Plymouth Sound with a depth of 51 m. The locations of both sites are shown in Figure 2. Environmental conditions at both sites were analysed and applied to their respective platforms to evaluate mooring system performance under real-world conditions.

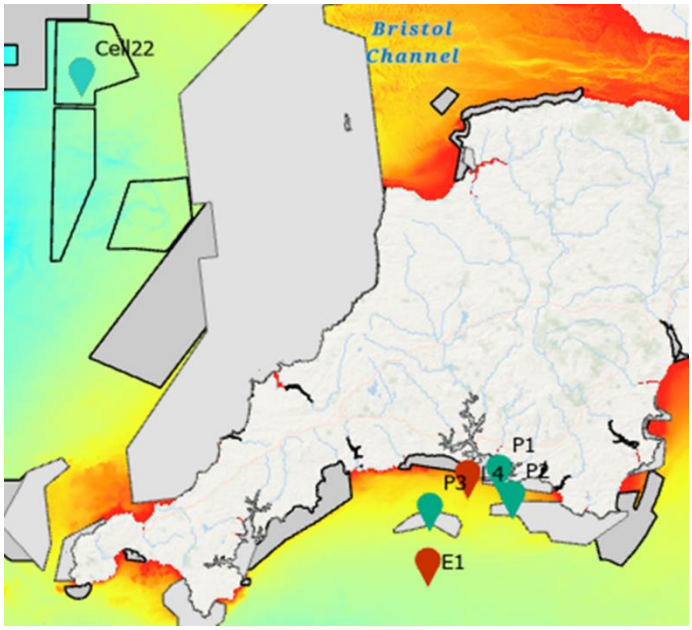

Figure 2 The cell22 and L4 location

Wave data (significant wave height H_s, peak wave period T_p, and mean wave direction Dir_m) was obtained from the UK Met Office wave hindcast product(Graham et al., 2018), with a 3-hour temporal and 1.5 km spatial resolution. Wind data (10 m u-component and v-component of wind) was sourced from ERA5 reanalysis (Hersbach et al., 2020)at hourly temporal and 0.5° spatial resolution, while current data (northward sea water velocity U_y and eastward sea water velocity U_x) came from the Atlantic-European North West Shelf Ocean Physics reanalysis at hourly temporal and 7 km spatial resolution. Collected wind speed (at 10 m height) is transformed to the hub height (150 m) through the logarithmic profile for the environmental condition definition. Wave and wind data span 1980–2009 (30 years), while current data covers 2000–2019, all retrieved from the Copernicus Marine Environment Monitoring Service (http://marine.copernicus.eu/). The environmental conditions at both study sites were derived via spatial interpolation of these numerical model datasets. The rose plots showing the directional distribution of the wind speed, significant wave height and current speed of both sites are demonstrated in Figure 3.

Generally, Cell22 experiences a more energetic sea state than L4, though both sites share similar wave direction distributions, with waves predominantly coming from the west and spanning northwest to southwest. At Cell22, where the full-scale platform is located, wave heights frequently exceed 3.5 meters, indicating a high-energy offshore environment. In contrast, L4, the site of the ACTOR platform, experiences lower waves, generally below 2.5 meters, with a more concentrated southwest direction. Wind speed distributions also differ. Cell22 exhibits a broader range, with frequent occurrences above 10 m/s, mainly from the west and northwest. L4 follows a similar directional pattern but with overall lower wind speeds, and high-wind events are less frequent. Current speed at Cell22 is more variable, with a maximum speed of 0.816 m/s, whereas L4's currents are more directionally constrained

along the west-east axis, peaking at 0.743 m/s. For all loading cases in this study, the maximum current speed at each site is applied.

Since the ACTOR platform does not include a wind turbine, wind conditions are considered but not the primary focus for response assessment. Thus, wind-wave-current misalignment is not included, and all simulations assume aligned environmental loads. The characteristic sea states consider maximum current speed while varying wind and wave conditions.

To estimate extreme environmental conditions, environmental contours corresponding to different return periods are used. Among various contour generation methods, the Inverse First Order Reliability Method (IFORM) is widely adopted. This study applies the Direct-IFORM method(Mackay & de Hauteclocque, 2023), which accommodates higher-dimensional data without requiring a joint distribution model. Environmental contours are generated using the open-source tool from https://github.com/edmackay/Direct-IFORM. Thirty years (1980-2009) of wind and wave data were used to generate contours (see Figure 4), defining the design load cases (DLCs).

For extreme condition assessment, conditions along the left side of the 50-year return period contour were selected, as this region corresponds to maximum wave steepness (see Cases 01–08 in Table 1 and Table 2). In these cases, the wind turbine on the full-scale platform remains parked, ensuring the evaluation of structural integrity and response under peak loads, expected to occur once every 50 years.

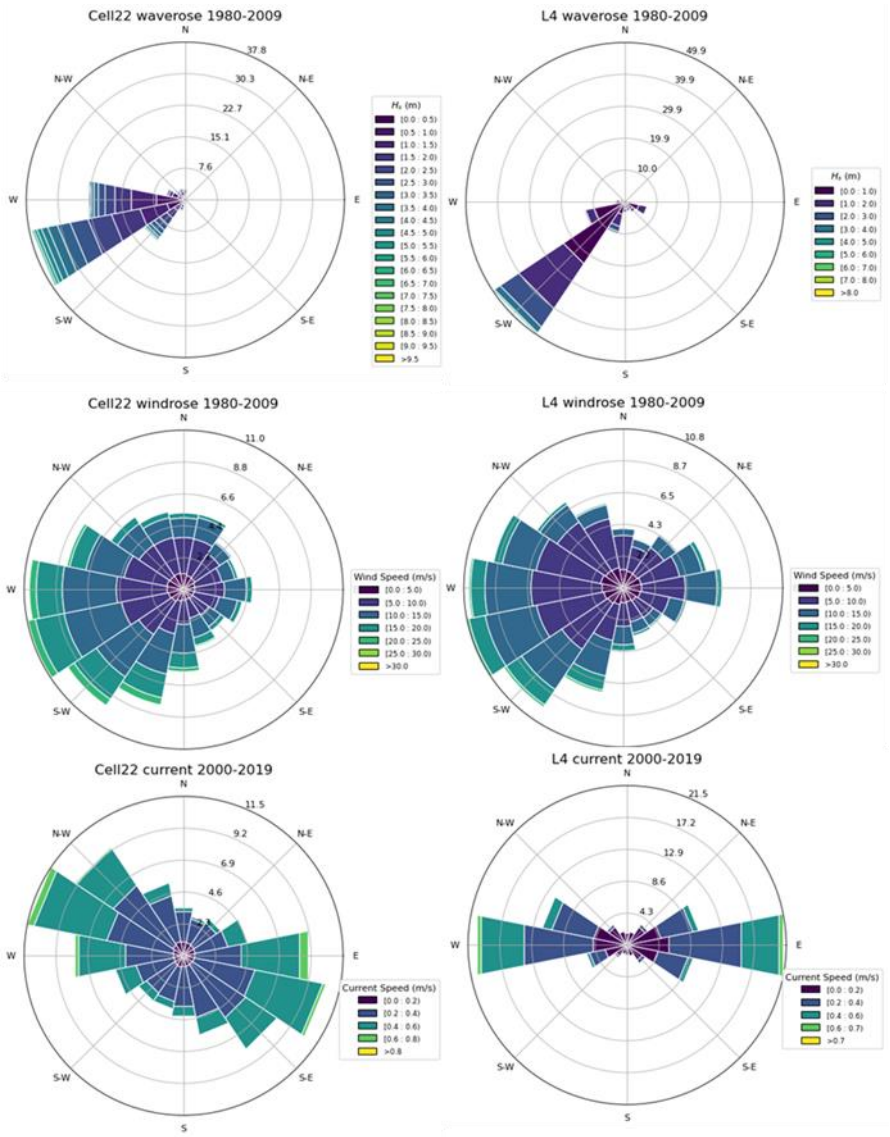

Figure 3 The rose plot of the wave, wind and tidal current condition for L4 and Cell22

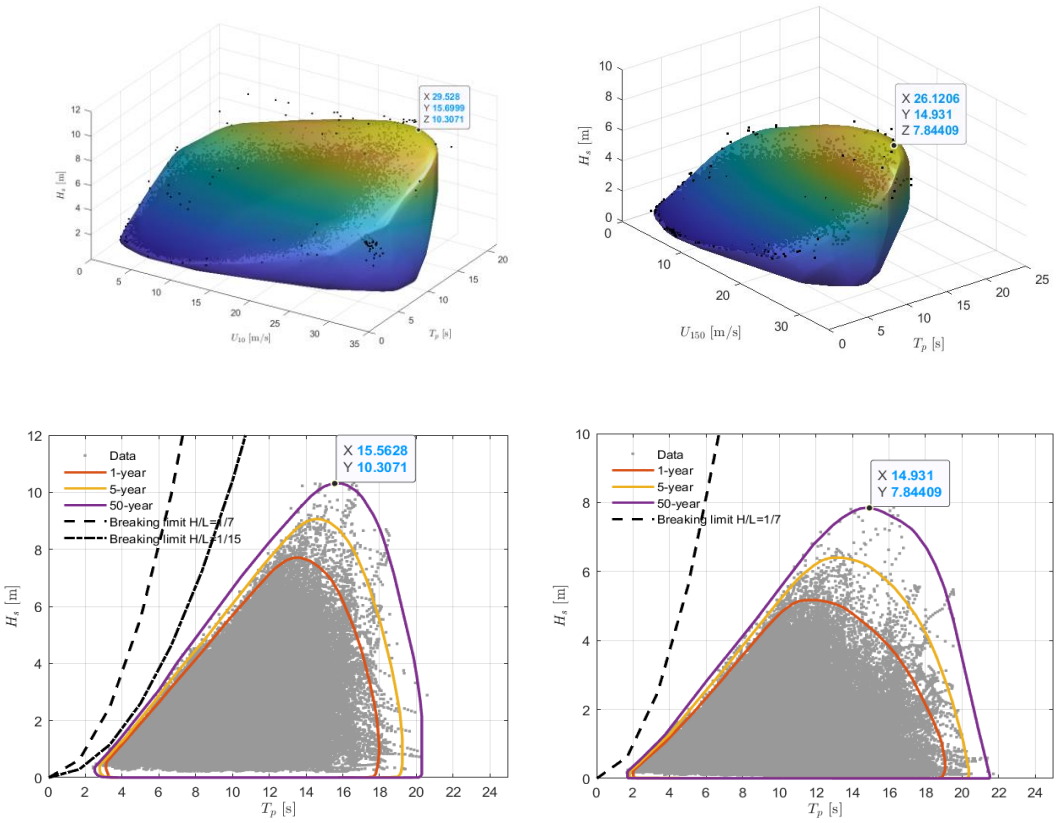

Figure 4 Extreme environmental contours associated with 50 year return periods of sea states represented by significant wave height, peak period and wind speed. Hindcast data at 3 h resolution between 1980 and 2019. The left top and left bottom shows the contours in 3D and 2D for Cell22 site, respectively, while the right top and right bottom shows the 3D and 2D contours for L4 site.

For fatigue analysis, operational conditions where the wind turbine is actively generating power are considered. The discrete scatter diagrams identifying sea states with an occurrence probability above 95% were selected (see Figure 5), corresponding to Cases 09–19.

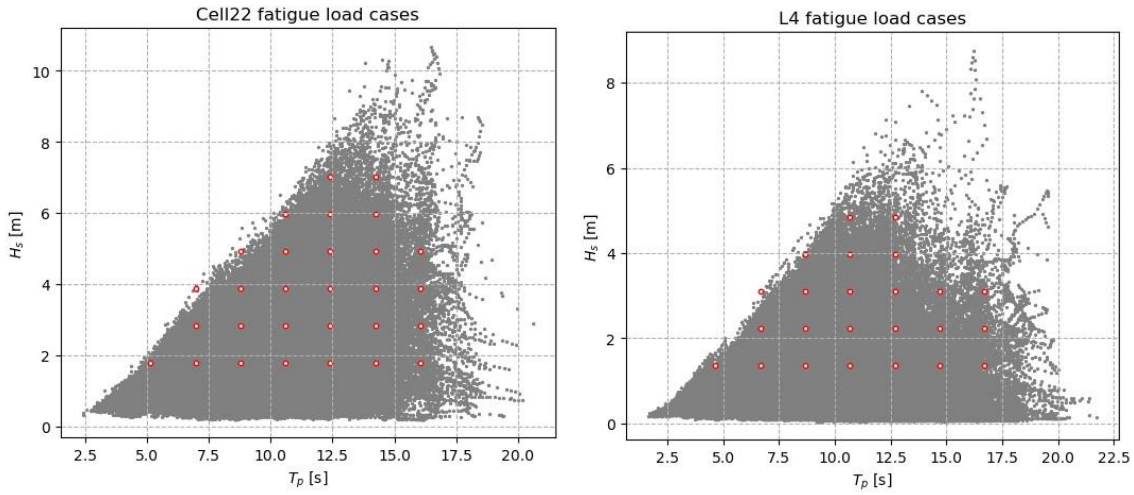

Figure 5 Discrete sea states for fatigue assessment

In the simulation times of all cases in this study are set to be 7200s, which aims to simulate the storm and operational conditions under the real world. The waves are defined by JOHNSWAP spectrum(Mazzaretto et al., 2022) with specified peak shape parameters (Gamma) in both sites.

Table 1 The environmental conditions in Cell22, wave, wind and current directions in Orcafelx are 180, 180 and 135

	Hs (m)	Tp (s)	Gamma	Wind (m/s) 150m	Tidal Current (m/s) on the surface	Occurrences in 11 years (counts/1000)
Case 01	10.3	15.56	3.3	29.528	0.816	
Case 02	6.155	9.549	3.76	25.605	0.816	
Case 03	7.355	11.036	2.92	27.443	0.816	
Case 04	8.39	12.19	2.49	25.809	0.816	
Case 05	9.441	13.637	1.91	29.231	0.816	
Case 06	9.327	17.462	1	26.9	0.816	
Case 07	8.509	18.13	1	21.264	0.816	
Case 08	7.134	18.778	1	21.18	0.816	
Case 09	1.78	10.60	1.00	20.63	0.816	99.34406
Case 10	1.78	6.97	1.00	22.08	0.816	75.48483
Case 11	1.78	8.79	1.00	22.16	0.816	74.20146
Case 12	1.78	5.15	3.69	22.48	0.816	54.70568
Case 13	1.78	12.42	1.00	18.78	0.816	52.11043
Case 14	2.82	10.60	1.00	24.80	0.816	45.51392
Case 15	2.82	8.79	1.00	23.28	0.816	43.83413
Case 16	2.82	12.42	1.00	23.52	0.816	37.2804
Case 17	2.82	6.97	2.66	31.16	0.816	35.48369
Case 18	3.87	10.60	1.00	26.46	0.816	25.0057
Case 19	3.87	12.42	1.00	25.95	0.816	21.50924

Table 2 The environmental conditions in L4, wave, wind and current directions in Orcafelx are 180, 157.5 and 135

	Hs (m)	Tp (s)	Gamma	Wind (m/s) 150m	Tidal Current (m/s) on the surface	Occurrences in 11 years (counts/1000)
Case 01	7.844	14.931	1	26.121	0.743	
Case 02	3.569	7.21	3.9	16.7	0.743	
Case 03	4.601	8.727	2.92	19.967	0.743	
Case 04	5.692	10.276	2.22	23.658	0.743	
Case 05	6.885	12.099	1.55	29.764	0.743	
Case 06	6.862	17.73	1	23.05	0.743	
Case 07	5.863	18.59	1	22.155	0.743	
Case 08	4.793	19.419	1	17.184	0.743	
Case 09	1.35	6.67	1.00	22.08	0.743	112.5257
Case 10	1.35	8.68	1.00	22.16	0.743	78.8444
Case 11	1.35	4.67	3.11	22.48	0.743	50.89551
Case 12	2.22	8.68	1.00	23.28	0.743	43.25234
Case 13	2.22	6.67	1.83	31.16	0.743	34.94182
Case 14	1.35	10.68	1.00	20.63	0.743	31.47102
Case 15	2.22	10.68	1.00	24.80	0.743	24.16439
Case 16	3.09	8.68	1.08	30.08	0.743	16.92049
Case 17	3.09	10.68	1.00	26.46	0.743	15.20648
Case 18	1.35	12.69	1.00	18.78	0.743	13.0105
Case 19	1.35	14.69	1.00	17.57	0.743	11.30789

Mooring Configurations for the Two Platforms

The mooring configuration for the full-scale platform consists of three chains, each characterized by uniform properties (shown by Figure 6). This mooring is designed for the deployment at 80 m water depth. The two front moorings primarily resist environmental loads such as wind, waves, and tidal currents, sustaining significant tensile stresses. They employ 105 mm R3 studless mooring chains, each of 550 meters long, deployed symmetrically from the platform's three outer columns at a depth of 14 m below the still water level. The rear chain, measuring 300 meters, experiences comparatively lower loads due to its positioning.

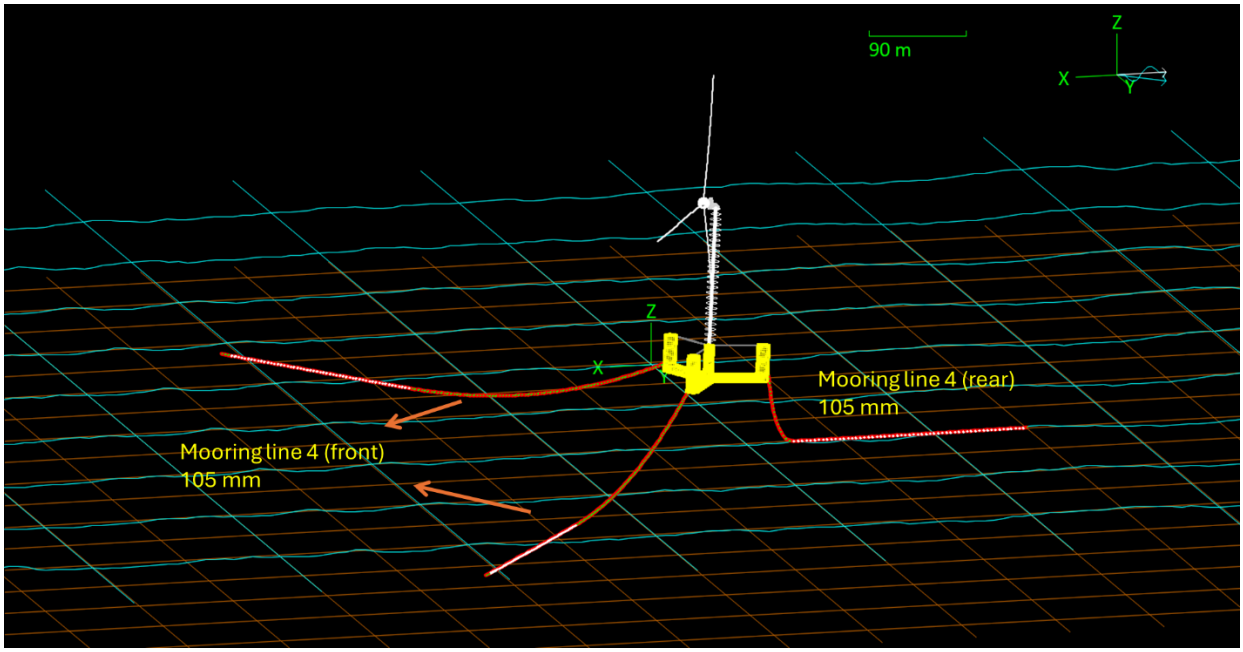

Figure 6 The mooring configuration of the 15MW offshore wind platform

Figure 7shows the mooring configuration of the ACTOR platform, with the test chains as the central components. This mooring is designed for the deployment at 51 m water depth. There are two main test chains (mooring line 1&4) shown in the diagram. The first test mooring line (mooring line 4) is designed to align with the direction of environmental loads, bearing most of these forces. It consists of two sections: the upper section, which connects to the centre bottom of platform, extends 180 m with a bar diameter of 105 mm, while the lower section, connecting the upper part to the seabed, extends 40 m with a bar diameter of 120 mm. The second test mooring line (mooring line 1) is oriented in the opposite direction of the first, connecting to the rear column centre bottom, counterbalancing the system. It extends 220 m with a bar diameter of 105 mm. Another key design objective of the second mooring line is to achieve the required pre-tension, ensuring the system's stability and intended operational conditions. To ensure the platform remains stable and secure, especially in the case of primary test chain failure, the configuration includes two additional safety chains, labelled as Mooring line 3 and 4. These chains follows the same direction as the two front chains of the prototype platform, each extends 300 m with a bar diameter of 50 mm. These are strategically employed

to safeguard the platform, effectively preventing unintended movement or total drift when the test chain is broken during the test. Table 3 lists details of the mooring line system.

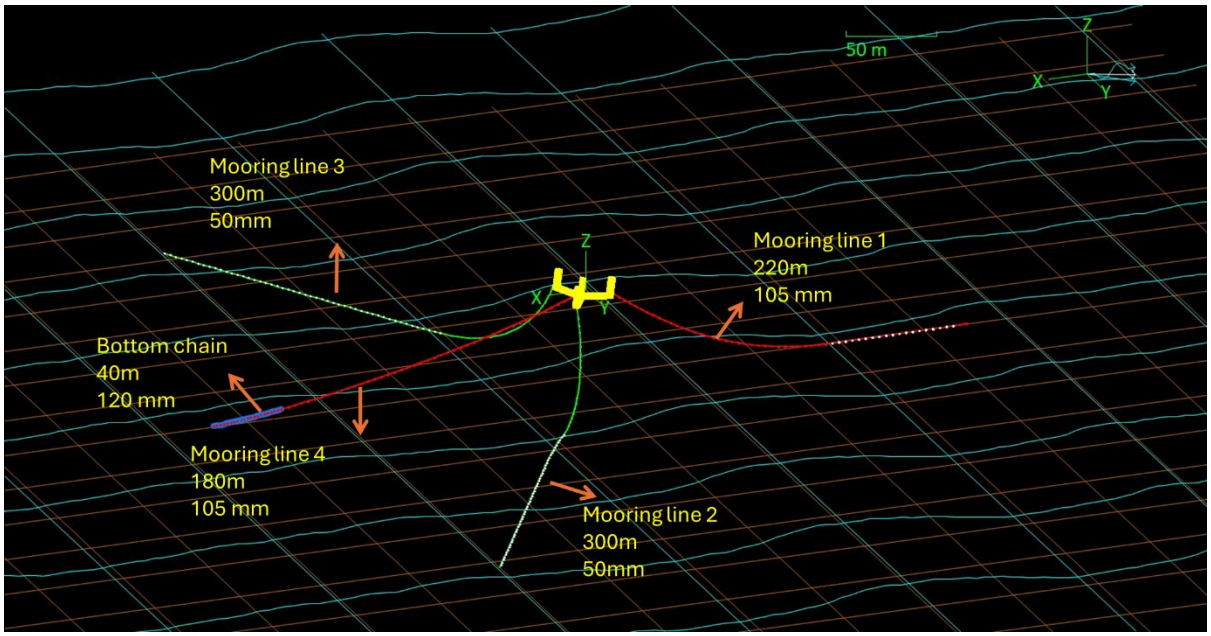

Figure 7 The mooring configuration of the ACTOR platform

Due to the ACTOR platform being situated in a milder sea environment, this mooring system is designed with a suitable level of pre-tension, ensuring that the test chain undergoes equivalent damage cycles and can be fully lifted to replicate peak load conditions observed in the full-scale platform. This ensures that the test chain's loading can encompass the extreme loads experienced in the full-scale platform. Additionally, the test chain can be fully lifted to accelerate fatigue testing. This dual emphasis on performance evaluation and safety highlights the stringent requirements of offshore engineering projects.

Table 3 The key information of the mooring lines

Mooring Line	Bar Diameter (mm)	Link Type	Weight (kN/m)	Pre-tension (kN)	Length (m)
Mooring Line 1 ACTOR	105	Studless	2.15	-	220
Mooring Line 4 ACTOR	105	Studless	2.15	640	180
Mooring Line 2&3 ACTOR	50	Studless	0.49	-	300
Bottom Chain ACTOR	120	Studdenlink	3.09	-	40
Mooring Line 4 Full scaled front	105	Studless	2.15	1644	550
Mooring Line 4 Full scaled front	105	Studless	2.15	1644	300

3. Analyse Approach and Methodology

This study employs time-domain numerical simulations using OrcaFlex (Orcina, 2024) to evaluate mooring system performance for both the full-scale and scaled platforms. Environmental conditions for extreme load and fatigue load have been defined in Table 1 and Table 2. Simulations are performed separately for both platforms, each subjected to environmental loading conditions specific to its proposed deployment site. Mooring configurations are adapted to reflect realistic constraints at each site, while maintaining comparable design intent. The ACTOR platform uses adjusted pre-tension and shallower water depth to induce elevated tension responses. Fatigue damage is estimated using rainflow counting and Miner's rule applied to time-domain tension histories.

By evaluating the frequency and magnitude of extreme loads and fatigue damage, this study assesses whether the ACTOR OffLab platform can serve as a reliable and conservative physical testbed for FOWT mooring system validation.

Extreme load analysis

The extreme load analysis focuses on Cases 01 to 08 for each site, examining the front mooring line tension on the full-scale platform and the test mooring line in the Actor model. The primary objective is to determine whether the ACTOR platform experiences the highest loading or even exceeds the loading conditions observed in the full-scale platform. These eight extreme cases are selected because they correspond to environmental conditions with a 50-year return period, ensuring that the analysis captures the most severe load scenarios that the platform may encounter. By evaluating multiple extreme cases, the study accounts for variations in wave, wind, and current conditions, leading to a more comprehensive understanding of peak loading behaviour.

To systematically analyse extreme loading, the process begins with data filtering, where instances of mooring line tension exceeding a predefined threshold are extracted. The threshold $T_{threshold}$ is defined as:

$$T_{threshold} = \frac{1}{2} T_{max}$$

where T_{max} is the highest recorded tension in the dataset. The filtered tension values are selected as:

$$T_{filtered} = \{T(t) | T(t) \geq T_{threshold}\}$$

After filtering, normalization is applied to scale the tension values relative to the maximum observed tension. The normalized tension $T^*$is given by:

$$T^* = \frac{T_{filtered}}{T_{max}}$$

This normalization ensures that all values fall within the range of 0 to 1, allowing for direct comparison across different cases and environmental conditions.

Once normalized, the data is categorized into bins for statistical evaluation. The binning process segments the tension values into intervals of fixed width ΔT^*,which in this study is set to 0.05. The bin index k for a given tension value $T^*$is calculated as:

$$k = \left\lfloor \frac{T^*}{\Delta T^*} \right\rfloor$$

where $\lfloor \cdot \rfloor$represents the floor function, ensuring that each value is assigned to the appropriate bin.

Finally, density estimation is performed to analyse the distribution of extreme tension values. The probability density function (PDF) $f(T^*)$ is approximated using a kernel density estimation (KDE) method:

$$f(T^*) = \frac{1}{nh} \sum_{i=1}^{n} K\left(\frac{T^* - T_i^*}{h}\right)$$

where $K(\cdot)$is the kernel function, $h$is the bandwidth, and n is the number of data points. This density function provides insight into how frequently different tension levels occur under extreme conditions.

By comparing the density distributions of mooring line tensions from the full-scale platform and the ACTOR platform, the analysis assesses whether the test environment successfully captures the extreme loads expected in real-world conditions. A agreement between these distributions indicates that the scaled testing provides an accurate representation of full-scale extreme loading behaviour, validating the methodology used in the study.

Fatigue analysis

Fatigue analysis in this study is conducted using two computational approaches, both based on rain flow cycle counting to evaluate the cyclic loading characteristics of the mooring system. These methods assess fatigue behaviour by identifying load cycles, computing stress ranges, and estimating cumulative fatigue damage.

The first method focuses on counting the occurrences of stress cycles, while the second evaluates fatigue damage using a T-N curve and Miner's rule. The analysis begins with data preprocessing, where the tension data is loaded, and a time column is defined. A filtering step is applied to select data within a specific time range to ensure consistency across different simulations. To identify cyclic loading patterns, peak and valley detection is performed. A key filtering criterion is applied, where only peaks and valleys with a tension difference greater

than 1 kN are considered. This threshold is set to remove fluctuations caused by numerical noise and small-scale oscillations that result from simulation errors rather than actual load cycles. While this approach effectively reduces irrelevant fluctuations, it is important to note that setting a fixed threshold, such as 1 kN, might inadvertently exclude low amplitude but genuine fatigue cycles. In cases where smaller stress cycles contribute significantly to fatigue damage accumulation, an adaptive threshold based on a percentage of the mean stress, or a statistical noise model could be a more refined approach. However, for this study, the 1 kN threshold provides a reasonable balance between filtering out numerical noise and retaining meaningful fatigue cycles. Once significant turning points are identified, rainflow cycle counting is applied to quantify stress cycles. This method iterates over the detected turning points, computing stress ranges and mean stresses for each cycle. A stack-based algorithm ensures that each turning point is either paired with a corresponding cycle or temporarily stored for future pairing, accurately modelling the fatigue behaviour of materials under repeated loading.

The second computational approach shifts focus to fatigue damage estimation by incorporating a T-N curve model. The damage calculation follows the standard fatigue damage accumulation approach using Miner's rule:

$$D = \sum_{i=1}^{n} \frac{n_i}{N_i}$$

where D is the cumulative damage, is the number of occurrences of stress cycle i, and $N_i$is the number of cycles to failure for the corresponding stress range, as defined by the T-N curve:

$$N = k\left(\frac{MBL}{\Delta S}\right)^{m}$$

where k and m are empirical fatigue parameters, MBL represents the breaking load of the mooring line, and ΔS the stress range for each identified cycle.

By combining cycle counting and fatigue damage estimation, this methodology provides a comprehensive assessment of the mooring system's fatigue performance. The first approach identifies the frequency of stress cycles, while the second evaluates the severity of damage, ensuring a robust analysis of fatigue life and potential failure points.

Mooring Chain design for ACTOR platform

Based on Table 2, ACTOR platform is expected to experience the most extreme environmental conditions under Case 01. Therefore, the time history results will be used to design the test chain (mooring line 4).

Results from these simulations are depicted in the time histories illustrated in Figure 8 and Figure 9 Back test chain (platform connection point). These figures specifically highlight the

maximum tension at the fairlead adjacent to the platform. The maximum tension of the mooring line 4 (3608kN) was recorded at 5920 seconds. Meanwhile, back test chain (mooring line 1) exhibited its maximum tension(2828kN) at 5915 seconds, displaying lower tension characteristics in comparison to the upwind lines.

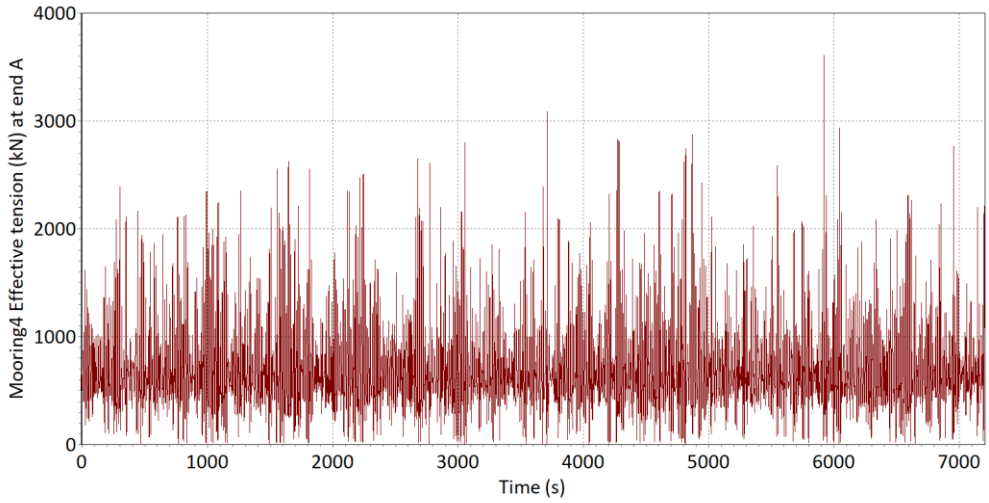

Figure 8 Front test chain (platform connection point)

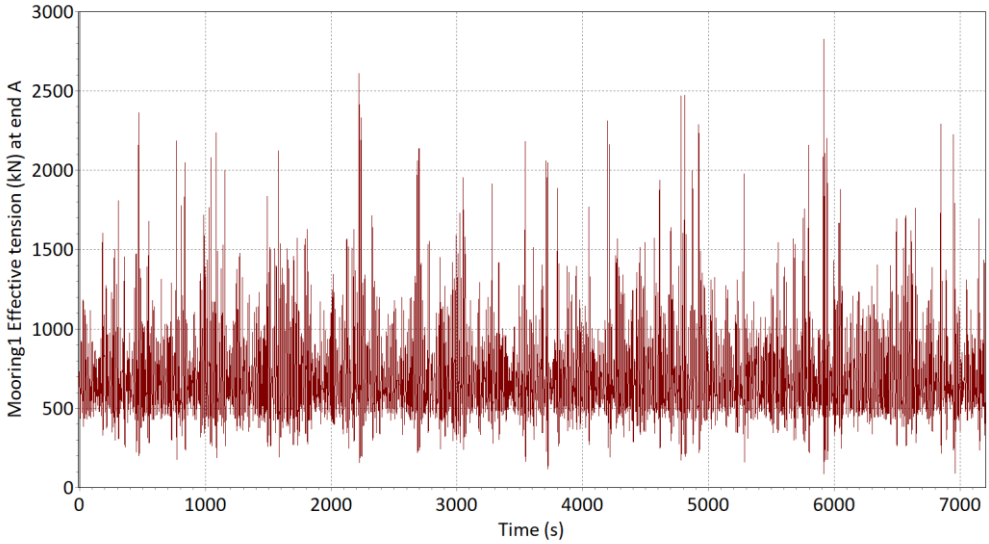

Figure 9 Back test chain (platform connection point)

During the simulations, both test chains were fully lifted, which may have increased fatigue on the mooring lines while accommodating the environmental loading levels typical of a full-scale platform. However, the safety line remained laid on the seabed, even in scenarios where the front test chain was absent. Figure 10 and Figure 11 depict the lift angles of both test chains, where it was noted that the angles of elevation were approximately 10 degrees for each chain. It should be noted that angles of -2 degrees and -178 degrees indicate that an anchor is lying flat along the seabed for the front and back test chains, respectively.

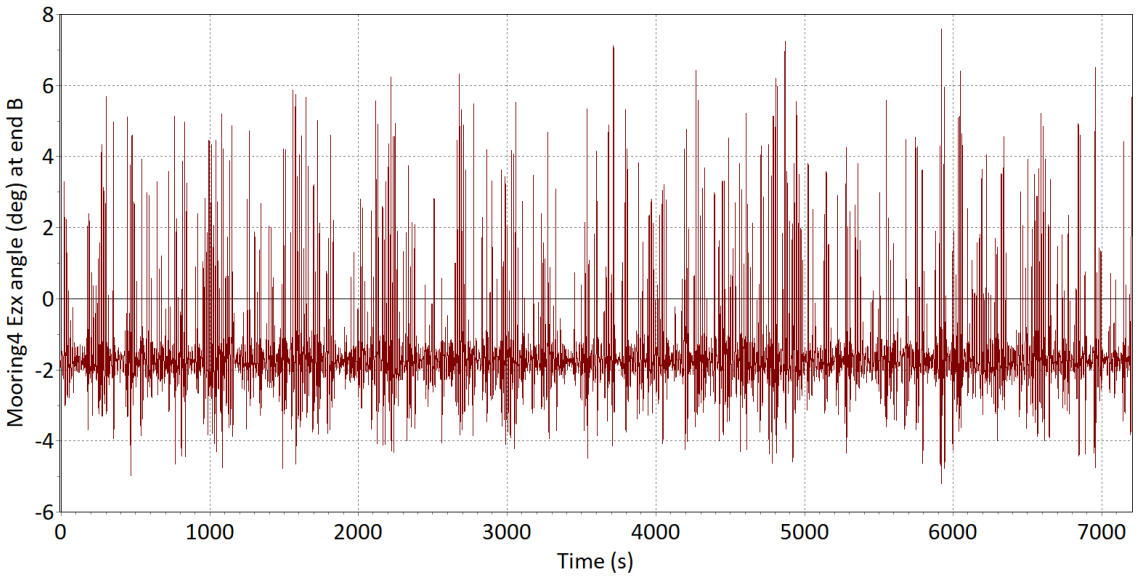

Figure 10 The lifted up degree on the anchor point of front test chain

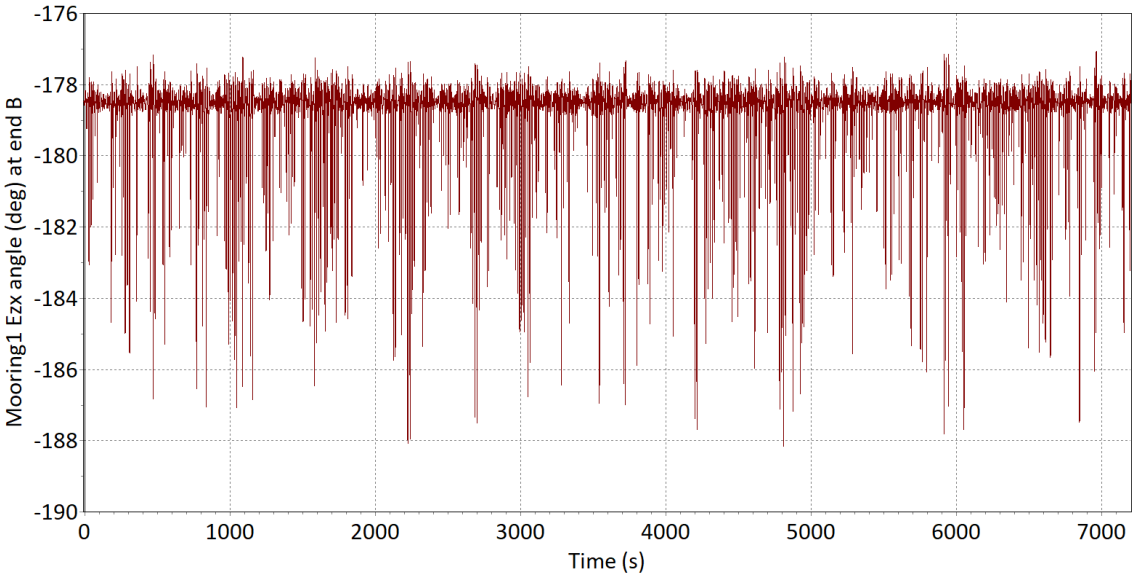

Figure 11 The lifted up degree on the anchor point of back test chain

The mooring design are sourced from industry-standard product catalogues, such as the Sotra Catalogue(Chain, 2021). A key element in the design process involves applying a safety factor (1.67) to the peak tension values derived from simulation data. Consequently, the MBL of each component must surpass this adjusted tension value to ensure reliability and safety. The components and their properties for the ACTOR platform mooring chains can be in Figure 12 to Figure 15 and Table 4 to Table 6.

Mooring line 4 (front test line)

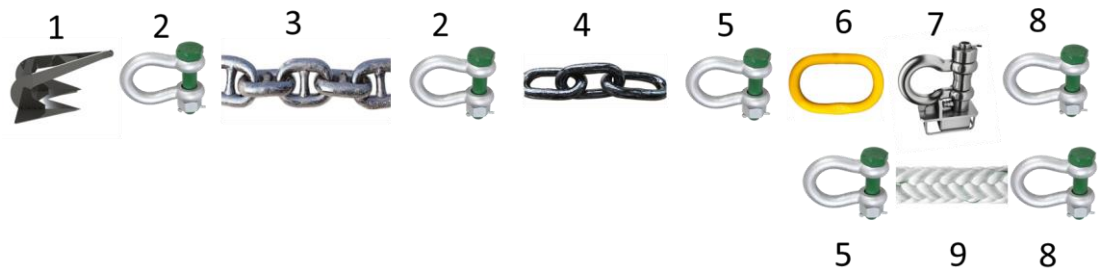

Figure 12 The front test chain components

Table 4 The front test chain components properties

Ref. No	Component name	Properties	Number	Length [m]	Comment
1	Anchor	Further design	1	NA	Pending
2	Bow shackle	WLL 4000 kN	2	NA	Suitable for 120 mm stud link chain
3	Bottom chain	MBL: 11140 kN, Proof loading: 7800kN Grade 3	1	40	120mm diameter needed for weight and test capacity of platform
4	Test chain	MBL: 6123 kN, Proof loading: 8753kN 105 mm Grade 3	1	180	105 mm diameter needed for full scaled platform
5	Bow shackle	WLL 4000 kN	2	NA	Connection of master link , load shackle and the safety line
6	Master link	WLL 4000 kN	1	NA	Connection of load shackle, redundancy line
7	Load shackle	WLL 4000 kN	1	NA	Measurement range based on the expected maximum loads
8	Bow shackle	WLL 4000 kN	2	NA	Connection to the platform to load shackle and safety line
9	Safety line	WLL 7000 kN	1	3	Redundancy line for load shackle

Mooring line 1 (Back test chain)

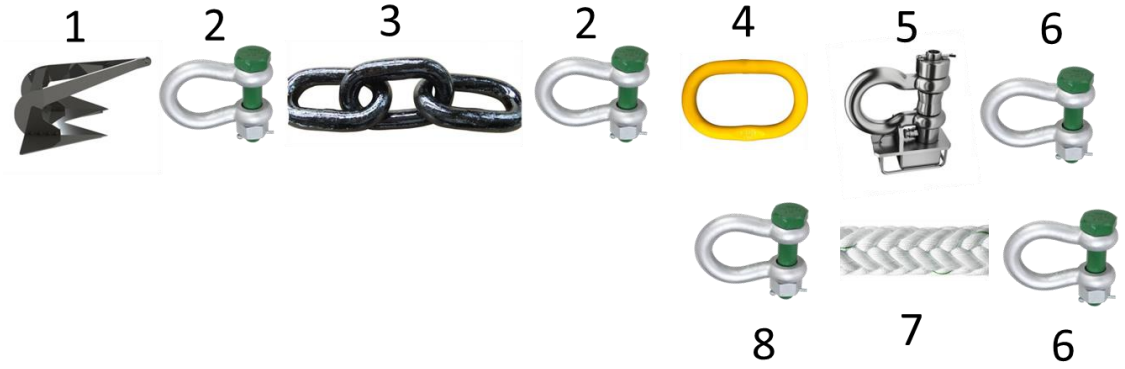

Figure 13 The back test chain components

Table 5 The back test chain components properties

Ref. No	Component name	Properties	Number	Length [m]	Comment
1	Anchor	Further design	1	NA	Pending
2	Bow shackle	WLL 4000 kN	2	NA	Suitable for 105 mm stud less chain
3	Test chain	MBL: 6123 kN, Proof loading: 8753kN 105 mm Grade 3	1	220	105 mm diameter needed for full scaled platform
4	Master link	WLL 4000 kN	1	NA	Connection of load shackle, redundancy line
5	Load shackle	WLL 4000 kN	1	NA	Measurement range based on the expected maximum loads
6	Bow shackle	WLL 4000 kN	2	NA	Connection to the platform to load shackle and safety line
7	Safety line	WLL 7000 kN	1	3	Redundancy line for load shackle
8	Bow shackle	WLL 4000 kN	1	NA	For connection of master link , load shackle and the safety line

Mooring line 2&3 (Safety chains)

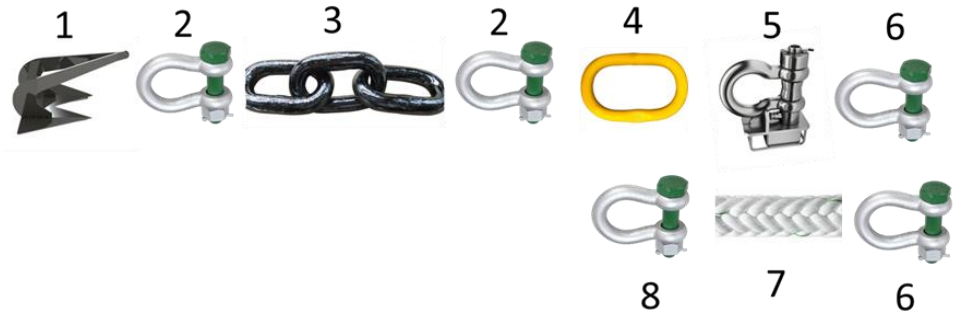

Figure 14 The safety chain components

Table 6 The safety chain components properties

Ref. No	Component name	Properties	Number	Length [m]	Comment
1	Anchor	Further design	1	NA	Pending
2	Bow shackle	WLL 1000 kN	2	NA	Suitable for 50 mm stud less chain
3	small chain	MBL:2230 kN, Proof loading: 1560kN 50 mm Grade 3	1	300	50mm diameter needed for weight
4	Master link	WLL 1000 kN	1	NA	Connection of load shackle, redundancy line

5	Load shackle	WLL 400 kN	1	NA	Measurement range based on the expected maximum loads
6	Bow shackle	WLL 1000 kN	2	NA	Connection to the platform to load shackle and safety line
7	Safety line	WLL 1000 kN	1	3	Redundancy line for load shackle
8	Bow shackle	WLL 1000 kN	1	NA	For connection of master link , load shackle and the safety line

4. Results and Discussions

Extreme load analysis

To assess the extreme loading conditions experienced by the mooring system, a statistical analysis was conducted on the tension distributions observed in the ACTOR platform and the full-scale platform, shown by Table 7. The objective of this analysis was to evaluate whether the scaled model effectively captures extreme tension events and to identify any significant discrepancies that may require further scaling refinements.

To provide a comprehensive assessment of extreme loads, results from Cases 01 to 08 were merged to form a unified dataset for analysis. This approach allows for a more statistically robust comparison between the ACTOR platform and the full-scale platform by incorporating a wide range of extreme loading conditions rather than focusing on isolated cases.

Table 7 The key statistical metrics of the mooring line4 in both ACTOR and Full scaled platform

	ACTOR platform	Full scaled platform
Mean (kN)	667.5551	1331.559
Maximum (kN)	3608.251	3544.378
Skewness	1.724388	0.2195
Kurtosis	6.288981	0.514281

Shown by Table 7, the mean tension in the full-scale platform was found to be significantly higher than in the ACTOR platform, with an average value of 1331.56 kN compared to 667.56 kN. This difference indicates that the full-scale platform experiences greater sustained loads, due to the hash environmental conditions at Cell22. However, the maximum tension values were similar, with 3608.25 kN recorded for the ACTOR platform and 3544.38 kN in the full-scale platform. The ability of the scaled model to reach peak loading conditions suggests that the pre-tensioning and mooring system adjustments effectively replicate extreme scenarios, even though the average tension remains lower.

While the ACTOR platform successfully reproduces peak loads, its load distribution exhibits significant differences from that of the full-scale platform. The skewness of the tension distribution in the ACTOR platform was calculated as 1.724, considerably higher than the 0.2195 skewness observed in the full-scale platform. The higher skewness in the ACTOR platform suggests that the mooring system in the scaled test is more sensitive to transient high loads, potentially due to localized environmental factors, mooring stiffness differences, or wave energy concentration effects.

Kurtosis further highlights the discrepancy in the frequency of extreme tension events between the two platforms. The ACTOR platform exhibited a kurtosis of 6.289, while the full-scale platform had a kurtosis of 0.514. A high kurtosis value suggests a leptokurtic distribution, meaning that extreme values occur more frequently than in a normal distribution.

To further investigate these differences, a PDF comparison was conducted (see Figure 15). The density distribution of the ACTOR platform exhibited a longer right tail, confirming that extreme high-tension values are more frequent. Conversely, the full-scale platform displayed a more compact and symmetric distribution, indicating that tension values are more evenly spread, with fewer extreme peaks. These findings align with the skewness and kurtosis results.

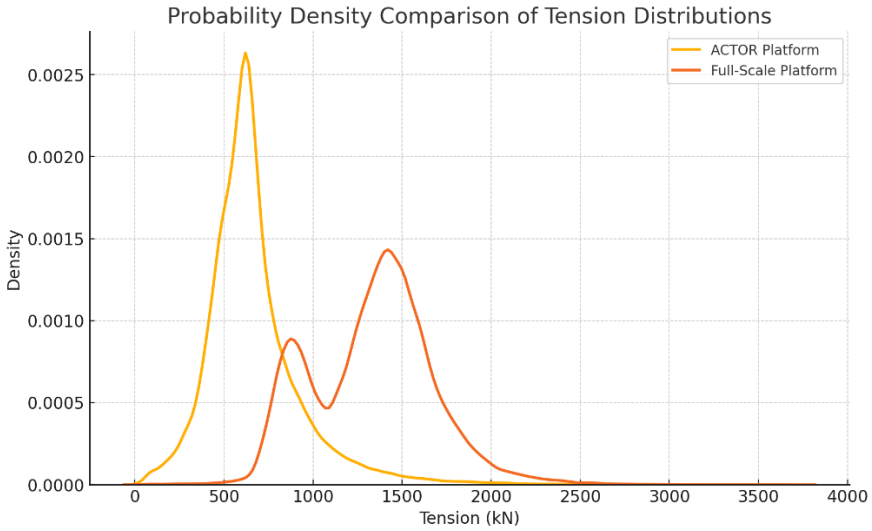

Figure 15 Probability density comparison of tension distributions between the ACTOR platform and the full-scale platform

Fatigue load analysis

The fatigue analysis first focuses on Case 09, which represents the highest occurrence scenario in the dataset. This case serves as a baseline for evaluating fatigue performance between the Full-Scaled platform and the ACTOR methodology, with a primary objective of determining whether ACTOR accelerates fatigue damage accumulation.

The analysis was conducted using tension data analysis, rainflow counting, and damage assessment. Rainflow counting analysis indicated that ACTOR exhibits a higher number of

cycles across all stress ranges, with a notable increase in high-stress cycles (>50 kN), as shown in Figure 16. The cycle distribution suggests that ACTOR induces more frequent fatigue loading, leading to accelerated fatigue damage.

As shown in Figure 17, the damage distribution shifts toward higher stress ranges (50-100 kN) in ACTOR, increasing the severity of fatigue loading. The Full-Scaled platform shows damage concentration in the 40-60 kN range, whereas ACTOR extends damage intensity into the 50-100 kN range, confirming that it accelerates fatigue failure. Higher stress ranges contribute significantly to fatigue damage accumulation in ACTOR, leading to reduced fatigue life

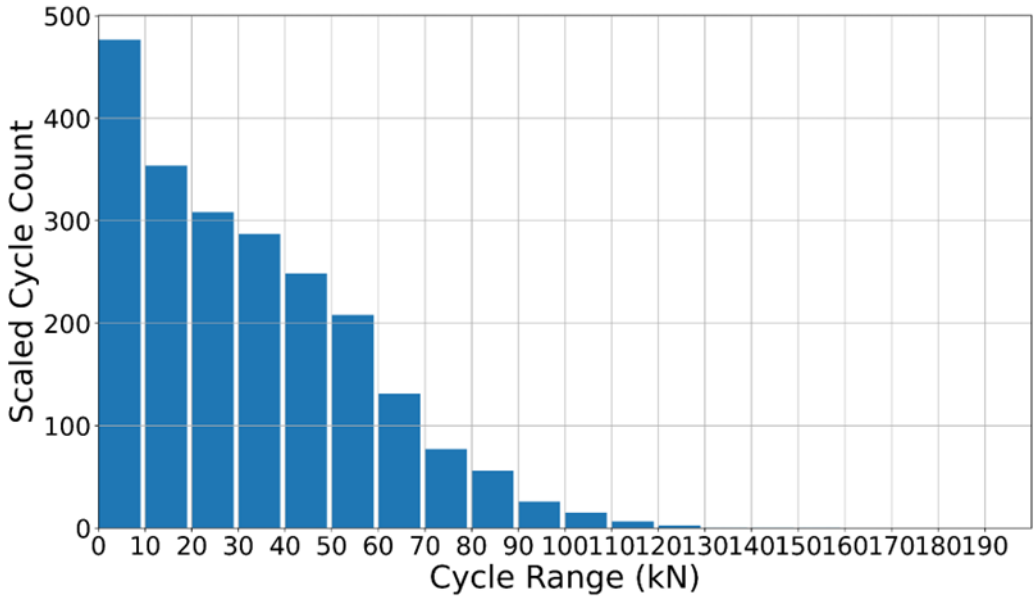

(a)

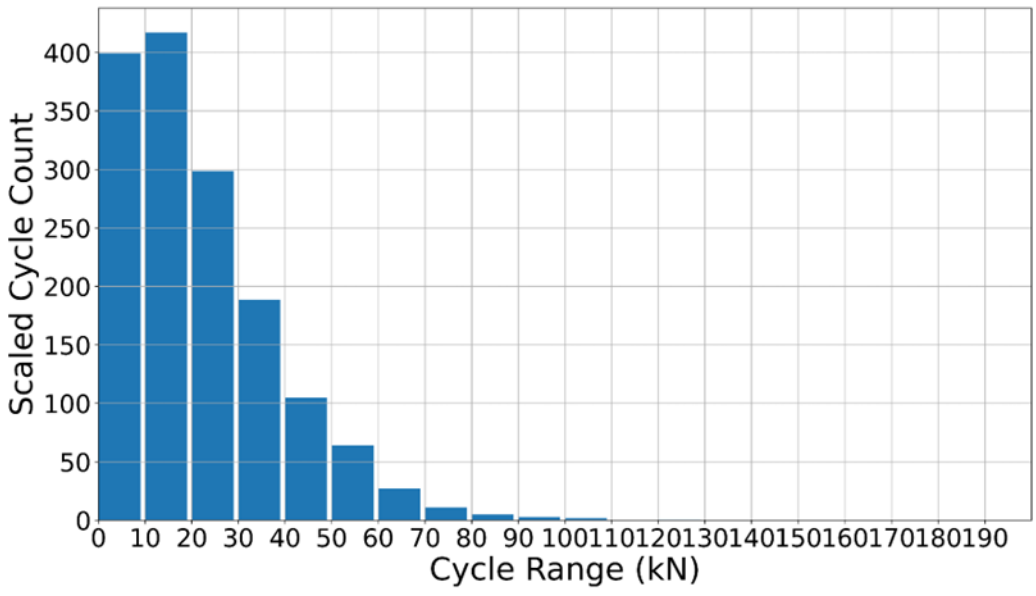

(b)

Figure 16 Rain flow counting in the case 09: (a) ACTOR platform, (b) Full scaled platform

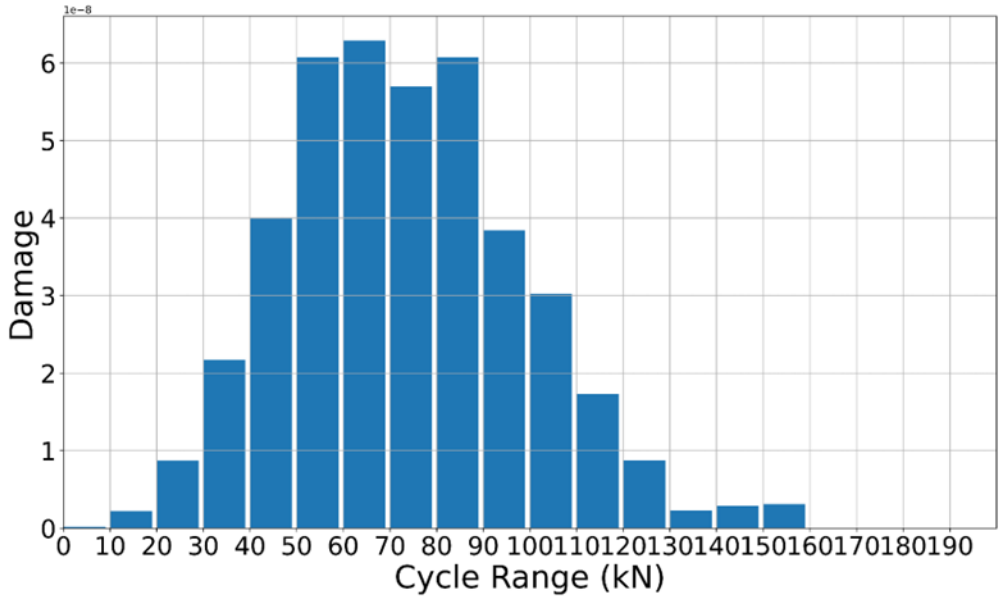

(a)

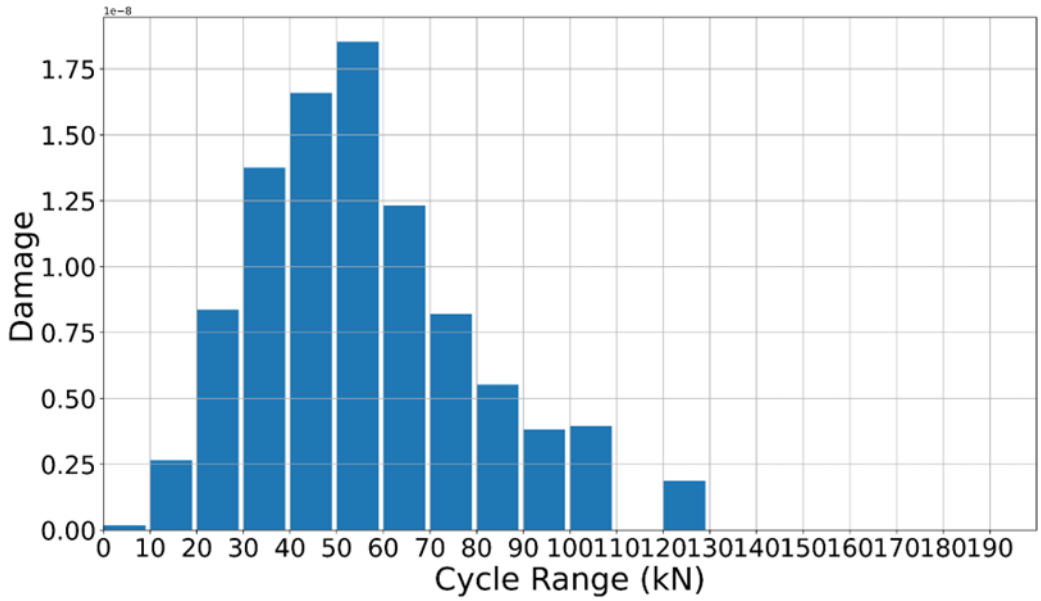

(b)

Figure 17 Rain flow damage in the case 09: (a) ACTOR platform, (b) Full scaled platform

While Case 09 provides critical insight into fatigue performance, real-world fatigue behaviour cannot be fully captured through a single-case study. Therefore, the analysis is extended to

Case 09-19, incorporating multiple scenarios with varying exposure times to better understand long-term fatigue trends.

The total exposure time for Case 09-19 over 11 years is 96,360 hours, with Full-Scaled cases accounting for 54,392 hours and ACTOR accounting for 41,632 hours, see Table 8. Although ACTOR has a lower total exposure time, its fatigue impact remains disproportionately high due to an increased cycle count and higher stress concentrations.

Table 8 The exposure time of case 09-19

	Full Scaled (hours)	ACTOR (hours)
Case 09	9572.79	10842.97
Case 10	7273.71	7597.446
Case 11	7150.05	4904.291
Case 12	5271.43	4167.795
Case 13	5021.36	3366.994
Case 14	4385.72	3032.548
Case 15	4223.85	2328.48
Case 16	3592.33	1630.458
Case 17	3419.20	1465.296
Case 18	2409.55	1253.691
Case 79	2072.63	1089.629
Total (case 09-19)	54392 (54.3%)	41632 (42%)
Total 11years hours	96360	96360

Rainflow counting analysis for Case 09-19 (see Figure 18)shows that ACTOR continues to exhibit a higher number of stress cycles across all ranges, with a notable increase in cycles above 50 kN. Compared to Case 09 alone, the broader dataset reveals a more comprehensive trend, confirming that ACTOR systematically increases fatigue loading across multiple cases.

The total fatigue damage comparison further validates this trend (see Figure 19). While Case 09 primarily shows peak damage accumulation between 50-70 kN, the merged analysis for Case 09-19 demonstrates a shift towards higher stress ranges (50-190 kN), intensifying fatigue severity. ACTOR's fatigue damage continues to increase at higher stress levels, whereas Full-Scaled damage remains concentrated in mid-range stresses.

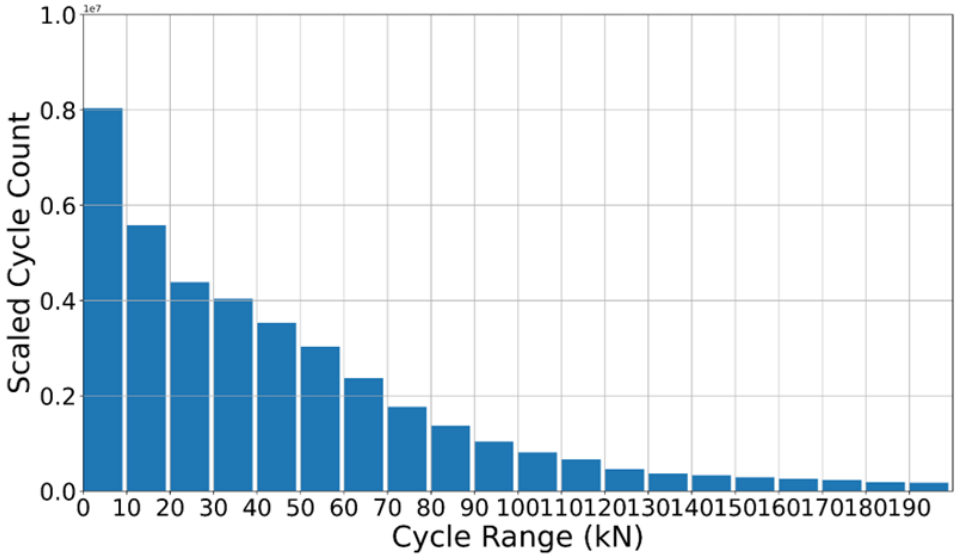

(a)

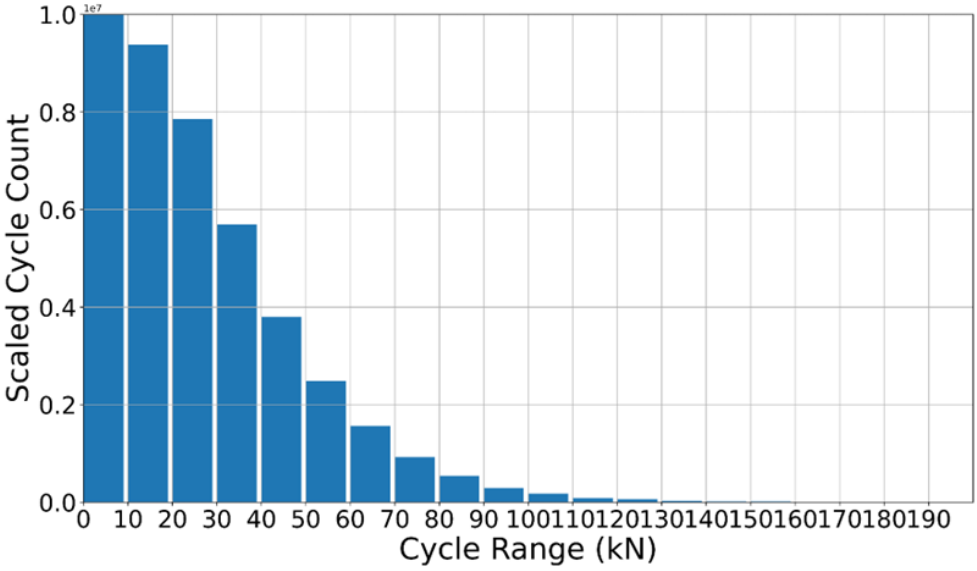

(b)

Figure 18 Rain flow counting in the case 09-19: (a) ACTOR platform, (b) Full scaled platform

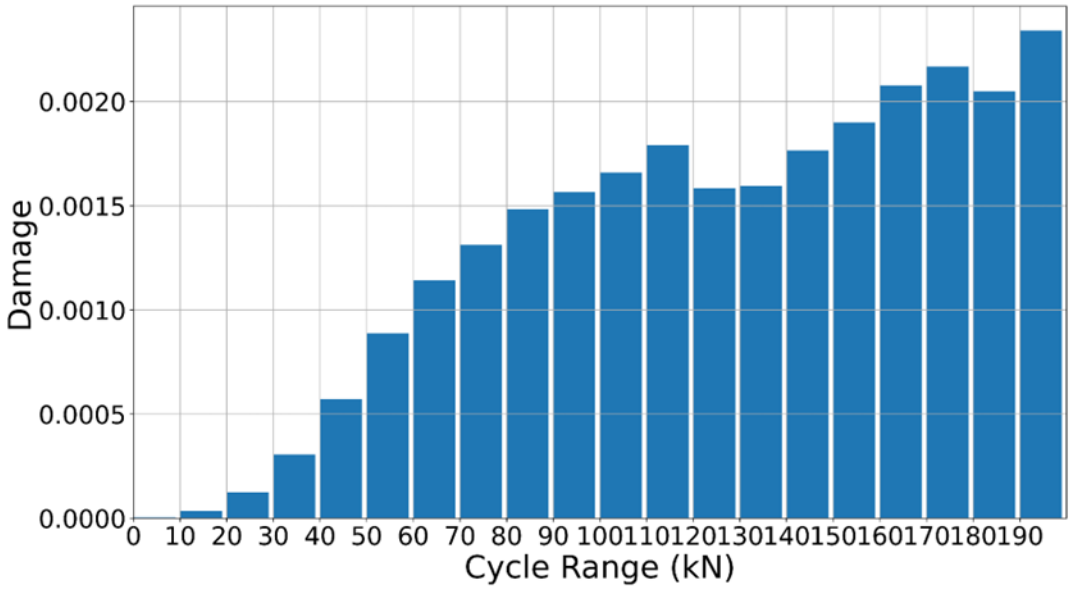

(a)

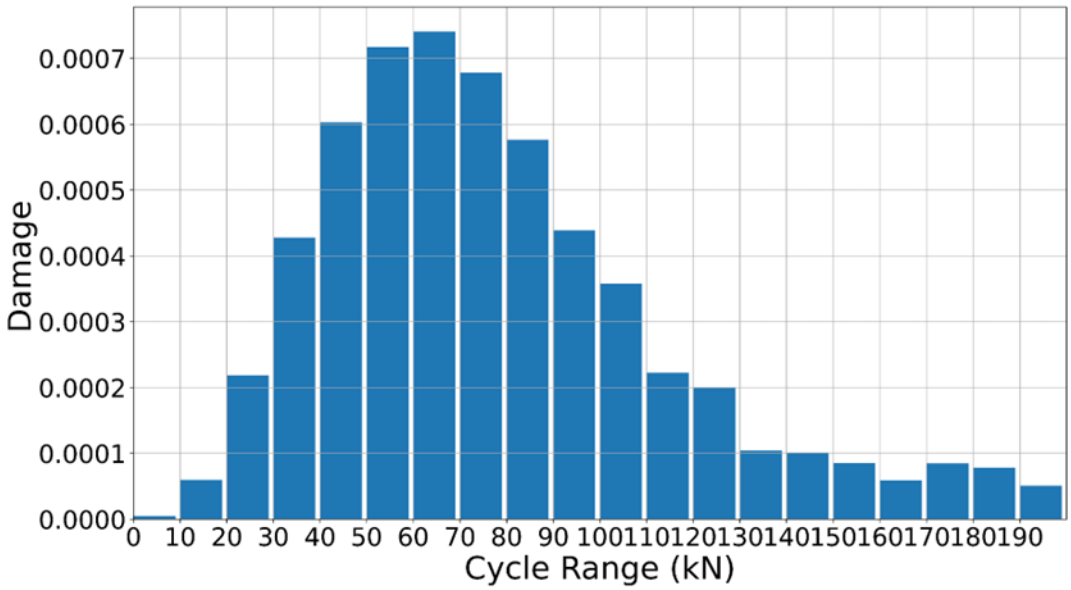

(b)

Figure 19 Rain flow damage in the case 09-19: (a) ACTOR platform, (b) Full scaled platform

Further extending the analysis, the fatigue life of mooring lines under both Full-Scaled and ACTOR conditions was evaluated. As shown in Figure 20, the full-scale platform exhibits a significantly longer mooring chain life than the ACTOR platform. In the full-scale platform, some portions of the mooring chain remain in contact with the seabed, which influences its fatigue performance in two keyways. First, seabed contact helps redistribute the load,

allowing a portion of the mooring line tension to be absorbed by the seabed rather than fully transmitted to the floating platform. This reduces dynamic stress variations in the upper sections of the mooring chain. Second, friction between the mooring chain and the seabed provides a natural damping effect, which dissipates energy from environmental forces and limits the frequency and amplitude of cyclic loading. Because of these combined effects, the full-scale mooring system experiences lower stress fluctuations, leading to fewer high-stress fatigue cycles and an estimated mooring line lifespan of approximately 63 years.

In contrast, the ACTOR platform allows the test mooring chains remain fully lifted from the seabed during testing. This intentional design choice was made to replicate extreme load conditions and accelerate fatigue accumulation within a controlled testing period. The absence of seabed contacts results in increased dynamic loading, as the mooring chains are fully exposed to wave and current-induced cyclic stresses. Additionally, because the chains are completely suspended, they experience higher stress ranges without the seabed's natural damping effect. This leads to frequent and high-amplitude load variations, significantly accelerating fatigue damage accumulation.

The rainflow cycle counting analysis again confirms that ACTOR experiences approximate 5.5 times higher fatigue damage accumulation compared to the full-scale platform. As a result, the expected fatigue life of the mooring system is drastically reduced from 63 years in the full-scale platform to approximately 11.6 years in the ACTOR platform. The findings demonstrate that while the ACTOR platform successfully replicates peak mooring loads, its accelerated fatigue behaviour provides valuable insights into long-term mooring performance, contributing to more efficient and cost-effective offshore wind technology validation.

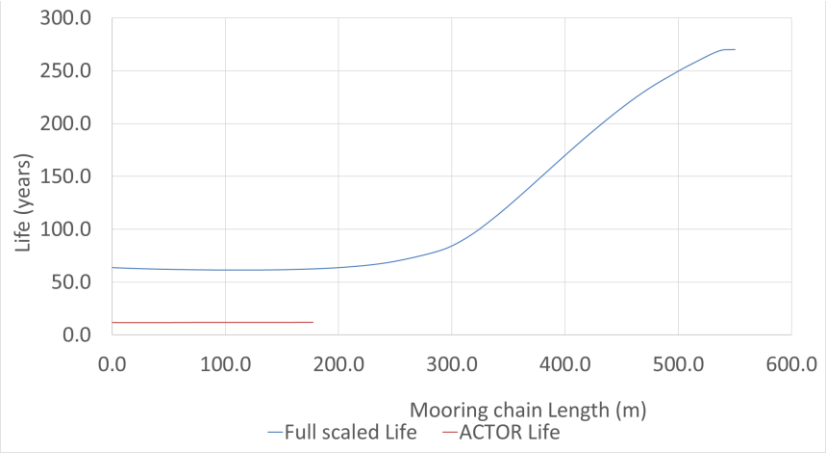

Figure 20 The mooring line life in both ACTOR and Full scaled platform

5. Conclusions

This study presented a comparative mooring analysis between a full-scale 15 MW floating wind turbine and a 1:3 scaled conceptual offshore laboratory platform (ACTOR), aimed at assessing its suitability as a conservative testbed for mooring system evaluation. The findings indicate that, despite being deployed in a nearshore site with milder environmental forcing, the ACTOR platform can replicate or exceed mooring tensions and fatigue accumulation observed in deeper offshore environments due to its shallow water depth and optimized pre-tension configuration. The main findings are summarized as follows:

- Extreme Load Validation: The extreme load analysis confirmed that, while the ACTOR platform operates in a reduced environmental force regime, The implementation of a suitable pre-tension level ensures that peak tension conditions are replicated while simultaneously accelerating fatigue damage accumulation. The peak mooring line tensions recorded were 3608 kN for the ACTOR platform and 3544 kN for the full-scale platform, indicating that the ACTOR system can effectively mimic full-scale extreme loading conditions. However, statistical analysis revealed differences in load distribution, with ACTOR exhibiting higher skewness (1.724) and kurtosis (6.289), suggesting more frequent transient extreme loads due to differences in environments and pre-tension.

- Fatigue Acceleration: The ACTOR platform significantly accelerates fatigue damage accumulation compared to the full-scale model. Rainflow cycle counting analysis showed that the ACTOR platform experienced round 5.5 times more fatigue damage, primarily due to the increased number of high-stress cycles exceeding 50 kN. The fatigue life estimation demonstrated a substantial reduction from 63 years (full-scale) to 11.6 years (ACTOR), confirming its ability to accelerate the assessment of long-term mooring durability within a compressed timeframe.

- Mooring Test Chain Design: Based on the Orcaflex simulations and industry information, a specialized test chain was designed for the ACTOR platform. The mooring chain components were selected based on simulated peak tension values with a safety factor of 1.67, ensuring structural integrity under testing conditions.

These results reinforce ACTOR's conceptual role as a bridge between numerical modeling and full-scale deployment. As a future step, physical construction and instrumentation of ACTOR will enable real-world validation of simulation results and further calibration of mooring response models. Once deployed, ACTOR will support accelerated life testing, sensor validation, and digital twin development for offshore renewable energy systems. Its accessibility, lower operational cost, and data-rich environment make it a valuable resource for de-risking offshore components and advancing floating wind technology readiness.

Future research will focus on improving environmental scaling methodologies, particularly in pre-tension adjustments, to further refine load distribution accuracy. Additionally, integrating real-time monitoring through digital twin technologies and expanding full-scale validation campaigns will strengthen the applicability of ACTOR findings to real offshore wind farms, ensuring more reliable and scalable offshore energy solutions.

Acknowledgements

We like to acknowledge the support through Innovate UK towards the WEDUSEA project [10103051] which sponsors the first author; support through EPSRC towards the ORE Supergen Hub [EP/S000747/1] which sponsored the second author; as well as support through the CIoS Good Growth fund towards the COMAC [BUS003_0112] project and the University of Plymouth that provided support through the OcEn project.

References

Allen, C., Viscelli, A., Dagher, H., Goupee, A., Gaertner, E., Abbas, N., Hall, M., & Barter, G. (2020). *Definition of the UMaine VolturnUS-S reference platform developed for the IEA wind 15-megawatt offshore reference wind turbine*.

Carpintero Moreno, E., Stratigaki, V., Troch, P., De Pauw, B., & Baur, T. (2020). Blue Accelerator: the new testing site in Ostend for maritime technology developments to enhance Blue Economy. General Assembly,

Chain, S. A. a. (2021). *Anchor and Chain Handbook 8th Edition*. https://www.sotra.net/contact/order-handbook/

Clark, D. S. B. A. J. B. R. (2024). *RISK ENGINEERING GUIDELINES FOR THE INSURANCE OF FLOATING OFFSHORE WIND FARMS* https://www.iua.co.uk/IUA_Member/Clauses/eLibrary/Clauses_Summary.aspx?DocumentKey=B508F167-C965-4707-9CE8-67EE124698ED

Dobson, T., Lenchine, V., & Bainbridge, S. (2024). A review on the interactions between engineering and marine life: key information for engineering professionals. *Journal of Ocean Engineering and Marine Energy*, *10*(2), 449-459.

Estate, T. C. (2023). *The Crown Estate refines plans for Celtic Sea floating wind | 2023—The Crown Estate refines plans for Celtic Sea floating wind*. https://www.thecrownestate.co.uk/en-gb/media-and-insights/news/2023-the-crown-estate-refines-plans-for-celtic-sea-floating-wind/

Gaertner, E., Rinker, J., Sethuraman, L., Zahle, F., Anderson, B., Barter, G., Abbas, N., Meng, F., Bortolotti, P., & Skrzypinski, W. (2020). Definition of the IEA 15-megawatt offshore reference wind turbine.

Graham, J. A., O'Dea, E., Holt, J., Polton, J., Hewitt, H. T., Furner, R., Guihou, K., Brereton, A., Arnold, A., & Wakelin, S. (2018). AMM15: a new high-resolution NEMO configuration for operational simulation of the European north-west shelf. *Geoscientific Model Development*, *11*(2), 681-696.

Hersbach, H., Bell, B., Berrisford, P., Hirahara, S., Horányi, A., Muñoz-Sabater, J., Nicolas, J., Peubey, C., Radu, R., & Schepers, D. (2020). The ERA5 global reanalysis, quarterly journal of the royal meteorological society.

Hmedi, M., Uzunoglu, E., Zeng, C., Gaspar, J., & Guedes Soares, C. (2023). Experimental challenges and modelling approaches of floating wind turbines. *Journal of Marine Science and Engineering*, *11*(11), 2048.

Mackay, E., & de Hauteclocque, G. (2023). Model-free environmental contours in higher dimensions. *Ocean Engineering*, *273*, 113959.

Matha, D., Schlipf, M., Pereira, R., & Jonkman, J. (2011). Challenges in simulation of aerodynamics, hydrodynamics, and mooring-line dynamics of floating offshore wind turbines. ISOPE International Ocean and Polar Engineering Conference,

Mazzaretto, O. M., Menéndez, M., & Lobeto, H. (2022). A global evaluation of the JONSWAP spectra suitability on coastal areas. *Ocean Engineering*, *266*, 112756.

McCoy, A., Musial, W., Hammond, R., Mulas Hernando, D., Duffy, P., Beiter, P., Perez, P., Baranowski, R., Reber, G., & Spitsen, P. (2024). *Offshore Wind Market Report: 2024 Edition*.

Orcina. (2023). *Comparison of loads from OrcaFlex and OpenFAST for the IEA 15 MW RWT*. https://www.orcina.com/wp-content/uploads/resources/validation/R15120101-OrcaFlex-15MW-RWT-Validation-Report.pdf

Shimada, S., Kogaki, T., Konagaya, M., Mito, T., Araki, R., Ueda, Y., & Ohsawa, T. (2022). Validation of near‐shore wind measurements using a dual scanning light detection and ranging system. *Wind Energy*, *25*(9), 1555-1572.

Timmington, D., & Efthimiou, L. (2022). Mooring Systems for Floating Offshore Wind: Integrity Management Concepts, Risks and Mitigation. World Forum Offshore Wind,

Touzon, I., Nava, V., Gao, Z., Mendikoa, I., & Petuya, V. (2020). Small scale experimental validation of a numerical model of the HarshLab2. 0 floating platform coupled with a non-linear lumped mass catenary mooring system. *Ocean Engineering*, *200*, 107036.

Tumse, S., Bilgili, M., Yildirim, A., & Sahin, B. (2024). Comparative Analysis of Global Onshore and Offshore Wind Energy Characteristics and Potentials. *Sustainability*, *16*(15), 6614.

Yang, R., Zheng, X., Chen, J., & Wu, Y. (2022). Current status and future trends for mooring systems of floating offshore wind turbines. *Sustainable Marine Structures*, *4*(2), 40-54.

Mooring Analysis in Offshore Floating Labs: Case Study on a 15MW Wind Platform

Chenyu Zhao [a], Jiaxin Chen [a,*], Lars Johanning [a]

[a] School of Engineering, Computing and Mathematics, University of Plymouth

Plymouth, Devon, United Kingdom. PL4 8AA.

[*] Corresponding author: Jiaxin.chen@plymouth.ac.uk

Abstract

As floating offshore wind turbines (FOWTs) expand into deeper and more complex marine environments, validating mooring system performance under real-world conditions becomes critical. This study investigates whether the purposely designed offshore floating laboratory (OffLab), named ACTOR, can serve as an effective and conservative testbed for mooring line evaluation. ACTOR is a conceptual platform inspired by the floater of the UMaine VolturnUS-S 15 MW semi-submersible FOWT design. The dimension of the ACTOR is about one third of the 15MW semi-sub floater and is intended deployment in a nearshore UK site with milder sea conditions. Using site-specific environmental data from two locations—the full-scale deployment zone in the Celtic Sea and a nearshore test location near Plymouth Sound—we perform comparative mooring analyses with OrcaFlex. Extreme load cases are defined using Direct-IFORM environmental contours, and fatigue conditions are derived from long-term wave spectral clustering. Results show that due to shallow water effects and tailored pre-tensioning, the ACTOR platform can replicate or exceed the mooring line tensions and fatigue damage accumulation observed in full-scale systems. The findings demonstrate the potential of ACTOR as a physically accessible, cost-effective platform for accelerated offshore component testing.

Keywords: Offshore Floating Laboratory, Mooring System, Extreme Load Analysis, Fatigue Testing, OrcaFlex

1. Introduction

Wind energy has experienced a remarkable evolution, transitioning from onshore installations to offshore developments, and progressively advancing from nearshore to far-offshore locations. This shift is driven by the stronger and more consistent wind resources found further from coastlines (Tumse et al., 2024). Offshore wind offers several advantages, including access to higher wind speeds and the ability to deploy larger turbines. In 2010, offshore wind capacity was a modest 3.1 GW, but by 2020, it

had expanded to 34.4 GW, reflecting a more rapid growth rate compared to onshore wind (McCoy et al., 2024). At the same time, this expansion of offshore wind energy into deeper waters has introduced significant challenges, particularly concerning the test of mooring systems for floating offshore wind turbines (FOWTs). Yang et al. (2022) gave a comprehensive review of the mooring system design for the FOWTs and pointed out the future research trends would focus on the more complex hybrid configurations and new materials.

However, above new trend may bring more challenges during the mooring line testing process. One primary challenge is achieving accurate scaling in physical models. Testing often involves scaled-down versions of mooring systems in wave basins or flumes. Maintaining geometric, kinematic, and dynamic similarity requires careful adherence to scaling laws, such as Froude scaling for gravitational forces. Some phenomena, like viscous effects, do not scale linearly, leading to discrepancies between model tests and real-world behaviour. This necessitates the use of advanced materials and techniques to mimic the properties of full-scale mooring lines accurately (Hmedi et al., 2023; Matha et al., 2011). Replicating the harsh and variable ocean conditions in a laboratory is another significant hurdle. Mooring lines in operational settings are subjected to complex loading from wind, waves, and currents. Creating a controlled environment that accurately simulates these combined forces is challenging (Timmington & Efthimiou, 2022). The final critical consideration is the fatigue of the mooring line. Accurately replicating these dynamic loads in testing environments is challenging but essential for assessing the long-term performance of mooring systems. However, the fatigue tests are always dry test which cannot fully consider the mooring line corrosion in the sea water(Matha et al., 2011).

This transition also introduces new financial and operational risks, particularly in the context of insurance coverage for floating wind technologies. Insurers assess offshore wind projects based on their technology readiness level (TRL) and historical performance data. Given that dynamic mooring systems, floating substations, and high-voltage export cables remain in the early stages of full-scale deployment, insurance premiums and risk mitigation strategies are critical concerns. Floating wind projects face higher estimated maximum loss (EML) scenarios, particularly due to potential failures in mooring integrity, power transmission systems, and extreme weather exposure. These risks can lead to significant delays and financial losses, making early-stage testing and validation essential for securing cost-effective insurance policies (Clark, 2024).

Offshore laboratories (OffLabs) offer a middle ground between numerical modelling and full-scale deployment, enabling controlled yet realistic testing of floating wind components. Examples include HarshLab 2.0 (Touzon et al., 2020), Blue Accelerator (Carpintero Moreno et al., 2020), and OCG-DATA (Dobson et al., 2024). This study introduces ACTOR, an Offshore Floating Laboratory currently under development in the southwest UK. With the Crown Estate's targeting the development of FOWT projects in the Celtic Sea by 2030 (Estate, 2023), the demand for such an OffLab has

intensified to de-risk essential components and sub-systems before at-sea testing. Based on a 1/3-scale version of the UMaine VolturnUS-S 15MW platform (Allen et al., 2020), ACTOR is designed to evaluate mooring system performance under real sea conditions. Unlike FOWTs, it does not include a wind turbine but is instead tailored for experimental testing of mooring lines, cables, sensors, and structural response in a nearshore environment.

Due to the differences in scale and target deployment areas—deep offshore sites for FOWTs versus nearshore locations for OffLabs—environmental loading differs significantly. However, because mooring systems rely on suspended weight for restoring force, the OffLab moorings may experience higher loads due to shallower water and increased stiffness. ACTOR is not a miniature turbine model; it is a sea-going laboratory for full-size mooring and cable components. The purpose is to expose real chains, connectors and terminations to the ultimate line tensions they would encounter offshore and to accelerate fatigue under seawater conditions. Strict Froude scaling would reduce loads and force the use of scaled components whose materials and wear mechanisms differ from the product of interest. By operating near shore and adjusting pre-tension, ACTOR reproduces the required offshore peak tension—and, by design, can be set to slightly exceed it—so that survival on ACTOR is a conservative indicator of survival offshore. The same pre-tension control increases stiffness and chain lift, shortening the time needed to observe fatigue damage while preserving the physical mechanisms (corrosion-fatigue, fretting, bedding-in) that laboratory factors alone cannot reproduce.

This study presents a comparative mooring analysis between the full-scale 15MW FOWT and the ACTOR platform (Figure 1), using OrcaFlex (Orcina, 2024) simulations to evaluate their respective responses to extreme and fatigue environmental conditions. The ACTOR platform is currently a conceptual design, and no physical deployment has occurred. The primary goal is to assess its effectiveness as a testbed by comparing load magnitudes, frequency of extreme events, and fatigue accumulation to those in full-scale deployment. Key research questions include:

1. Can an OffLab (ACTOR) effectively generate extreme mooring line tensions comparable to those of a full-scale offshore wind platform under different sea condition?
2. Does the ACTOR platform accelerate fatigue damage through pre-tension alteration?
3. What are the key differences in load distribution, frequency of transient extreme events, and fatigue damage accumulation between the OffLab and full-scale platforms?

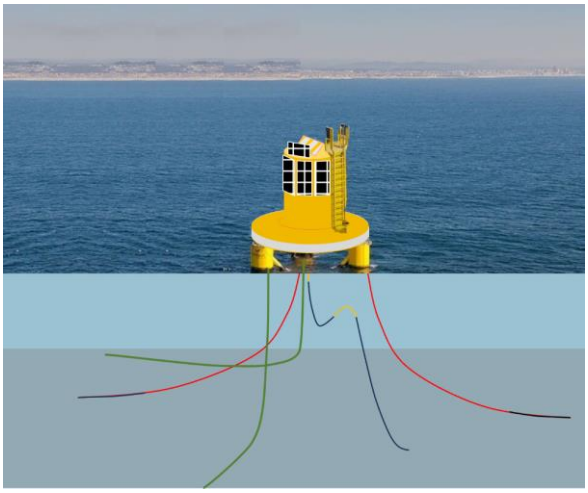

Figure 1 Conceptual illustration of the ACTOR OffLab platform. The topside is inspired by the HarshLab and adapted for visualisation purposes.

The remainder of this paper is structured as follows: Section 2 presents the case study development, detailing the full-scale and ACTOR scaled platforms, mooring configurations, and environmental conditions. Section 3 describes the analytical approach, including extreme load analysis, fatigue assessment, and mooring chain design. Section 4 provides results and discussions, comparing the mooring system performance of the two platforms under various environmental conditions. Finally, Section 5 concludes the study by summarizing key findings, validating the ACTOR platform's effectiveness, and suggesting future research directions.

2. Case study development

To investigate the feasibility of using the scaled OffLab ACTOR for mooring system evaluation, two representative platforms and deployment sites were selected. The full-scale reference platform is the UMaine VolturnUS-S (Allen et al., 2020), a 15 MW floating wind turbine with a three-column semi-submersible hull, designed for deep offshore deployment in the Celtic Sea. The scaled experimental platform (ACTOR) is derived from this reference design with a 1:3 geometric and mass scaling factor. While the ACTOR platform omits the wind turbine and tower components, it preserves the primary structural layout and mooring design principles to allow for focused testing of mooring line response.

The ACTOR platform is intended for nearshore deployment at Smart Sound Plymouth, an area with established monitoring infrastructure and easier access for operations. In contrast, the full-scale platform is hypothetically deployed at a Celtic Sea location aligned with the Crown Estate's Project Development Areas (PDAs) (Estate, 2023). These two sites differ significantly in environmental conditions, particularly water depth and wave climate. However, shallow water induces increased mooring line stiffness and larger dynamic tension responses. This makes it plausible that ACTOR, despite

being in a milder met-ocean environment, could replicate or even amplify the mooring load conditions experienced offshore.

Scenario-Based Environmental Conditions

This Celtic Sea area has characteristic depth of 80 m. The ACTOR platform site is located near Plymouth Sound with a depth of 51 m. The locations of both sites are shown in Figure 2. Environmental conditions at both sites were analysed and applied to their respective platforms to evaluate mooring system performance under real-world conditions.

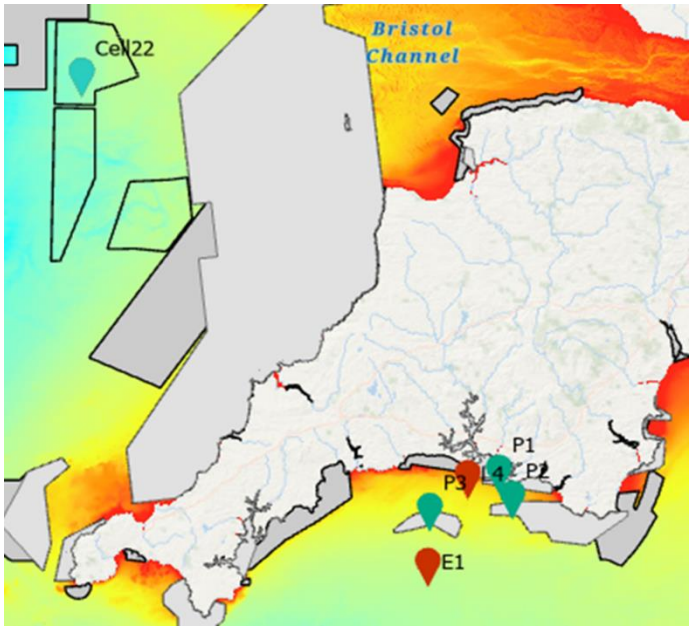

Figure 2 The cell22 and L4 location

Wave data (significant wave height H_s, peak wave period T_p, and mean wave direction Dir_m) was obtained from the UK Met Office wave hindcast product(Graham et al., 2018), with a 3-hour temporal and 1.5 km spatial resolution. Wind data (10 m u-component and v-component of wind) was sourced from ERA5 reanalysis (Hersbach et al., 2020)at hourly temporal and 0.5° spatial resolution, while current data (northward sea water velocity U_y and eastward sea water velocity U_x) came from the Atlantic-European North West Shelf Ocean Physics reanalysis at hourly temporal and 7 km spatial resolution. Collected wind speed (at 10 m height) is transformed to the hub height (150 m) through the logarithmic profile for the environmental condition definition. Wave and wind data span 1980–2009 (30 years), while current data covers 2000–2019, all retrieved from the Copernicus Marine Environment Monitoring Service (http://marine.copernicus.eu/). The environmental conditions at both study sites were derived via spatial interpolation of these numerical model datasets. The rose plots showing the directional distribution of the wind speed, significant wave height and current speed of both sites are demonstrated in Figure 3.

Generally, Cell22 experiences a more energetic sea state than L4, though both sites share similar wave direction distributions, with waves predominantly coming from the west and spanning northwest to southwest. At Cell22, where the full-scale platform is located, wave heights frequently exceed 3.5 meters, indicating a high-energy offshore environment. In contrast, L4, the site of the ACTOR platform, experiences lower waves, generally below 2.5 meters, with a more concentrated southwest direction. Wind speed distributions also differ. Cell22 exhibits a broader range, with frequent occurrences above 10 m/s, mainly from the west and northwest. L4 follows a similar directional pattern but with overall lower wind speeds, and high-wind events are less frequent. Current speed at Cell22 is more variable, with a maximum speed of 0.816 m/s, whereas L4's currents are more directionally constrained along the west-east axis, peaking at 0.743 m/s. For all loading cases in this study, the maximum current speed at each site is applied.

Since the ACTOR platform does not include a wind turbine, wind conditions are considered but not the primary focus for response assessment. Thus, wind-wave-current misalignment is not included, and all simulations assume aligned environmental loads. The characteristic sea states consider maximum current speed while varying wind and wave conditions.

To estimate extreme environmental conditions, environmental contours corresponding to different return periods are used. Among various contour generation methods, the Inverse First Order Reliability Method (IFORM) is widely adopted. This study applies the Direct-IFORM method(Mackay & de Hauteclocque, 2023), which accommodates higher-dimensional data without requiring a joint distribution model. Environmental contours are generated using the open-source tool from https://github.com/edmackay/Direct-IFORM. Thirty years (1980-2009) of wind and wave data were used to generate contours (see Figure 4), defining the design load cases (DLCs).

For extreme condition assessment, conditions along the left side of the 50-year return period contour were selected, as this region corresponds to maximum wave steepness (see Cases 01–08 in Table 1 and Table 2). In these cases, the wind turbine on the full-scale platform remains parked, ensuring the evaluation of structural integrity and response under peak loads, expected to occur once every 50 years.

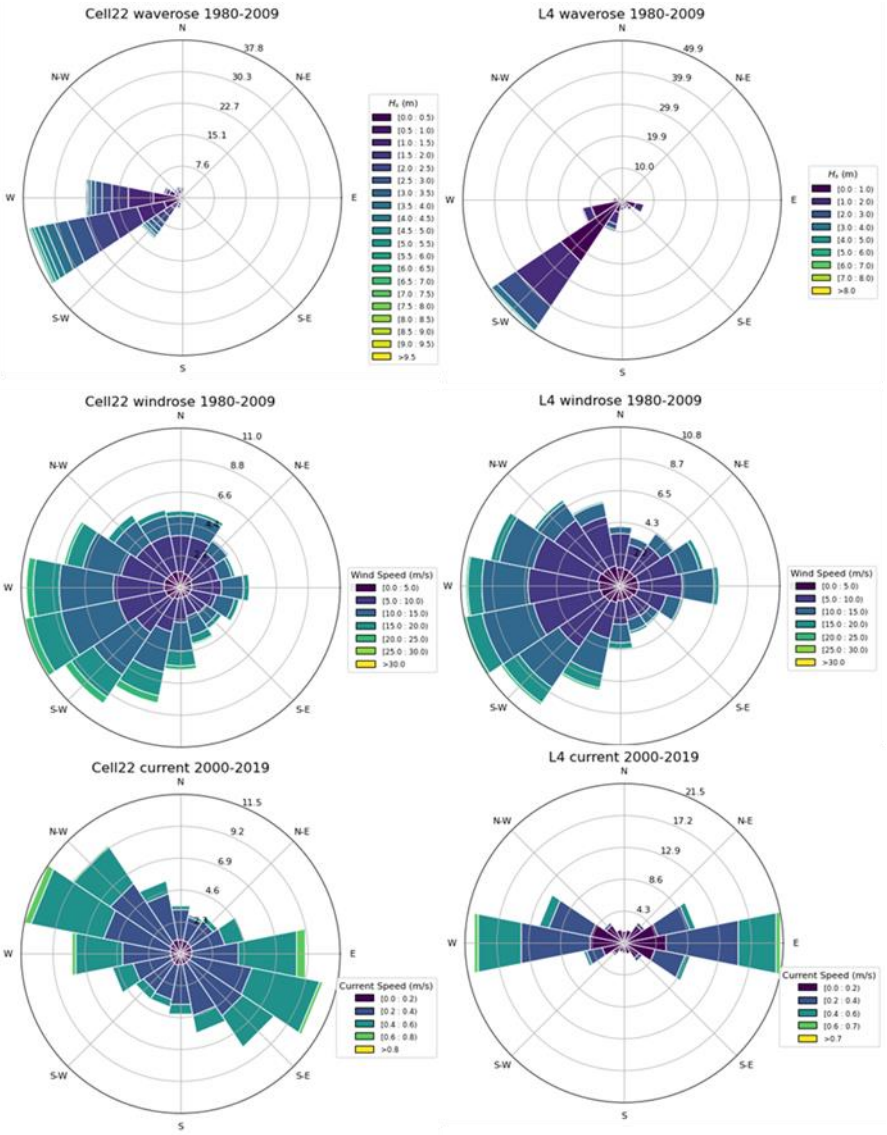

Figure 3 The rose plot of the wave, wind and tidal current condition for L4 and Cell22

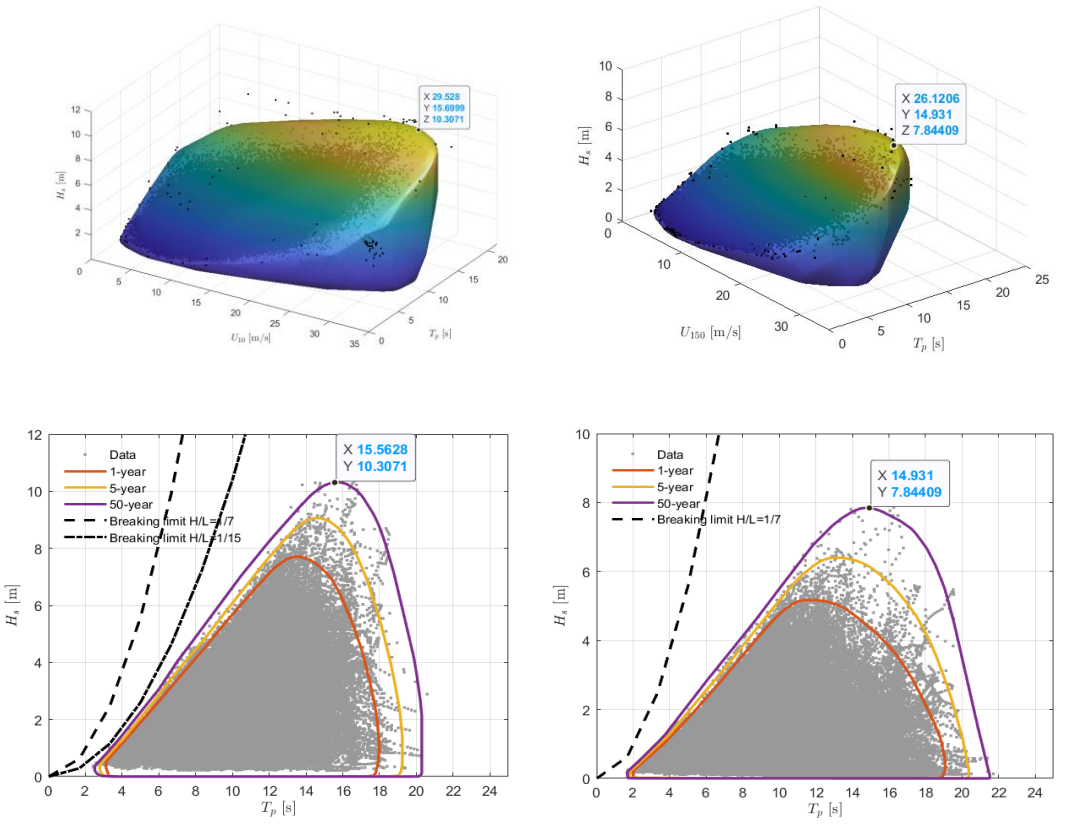

Figure 4 Extreme environmental contours associated with 50 year return periods of sea states represented by significant wave height, peak period and wind speed. Hindcast data at 3 h resolution between 1980 and 2019. The left top and left bottom shows the contours in 3D and 2D for Cell22 site, respectively, while the right top and right bottom shows the 3D and 2D contours for L4 site.

For fatigue analysis, operational conditions where the wind turbine is actively generating power are considered. The discrete scatter diagrams identifying sea states with an occurrence probability above 95% were selected (see Figure 5), corresponding to Cases 09–19.

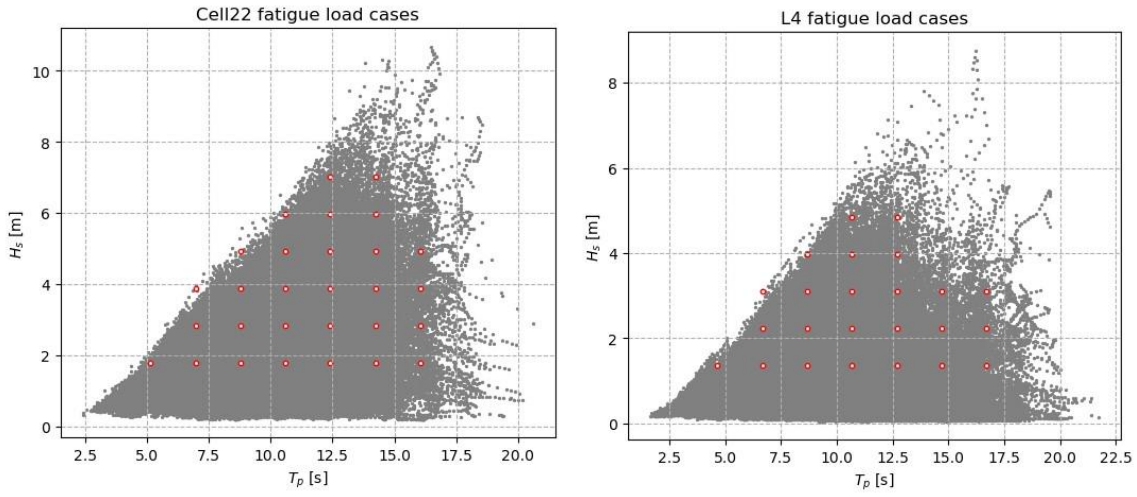

Figure 5 Discrete sea states for fatigue assessment

In the simulation times of all cases in this study are set to be 7200s, which aims to simulate the storm and operational conditions under the real world. The waves are defined by JOHNSWAP spectrum(Mazzaretto et al., 2022) with specified peak shape parameters (Gamma) in both sites.

Table 1 The environmental conditions in Cell22, wave, wind and current directions in Orcafelx are 180, 180 and 135

	Hs (m)	Tp (s)	Gamma	Wind (m/s) 150m	Tidal Current (m/s) on the surface	Occurrences in 11 years (counts/1000)
Case 01	10.3	15.56	3.3	29.528	0.816	
Case 02	6.155	9.549	3.76	25.605	0.816	
Case 03	7.355	11.036	2.92	27.443	0.816	
Case 04	8.39	12.19	2.49	25.809	0.816	
Case 05	9.441	13.637	1.91	29.231	0.816	
Case 06	9.327	17.462	1	26.9	0.816	
Case 07	8.509	18.13	1	21.264	0.816	
Case 08	7.134	18.778	1	21.18	0.816	
Case 09	1.78	10.60	1.00	20.63	0.816	99.34406
Case 10	1.78	6.97	1.00	22.08	0.816	75.48483
Case 11	1.78	8.79	1.00	22.16	0.816	74.20146
Case 12	1.78	5.15	3.69	22.48	0.816	54.70568
Case 13	1.78	12.42	1.00	18.78	0.816	52.11043
Case 14	2.82	10.60	1.00	24.80	0.816	45.51392
Case 15	2.82	8.79	1.00	23.28	0.816	43.83413
Case 16	2.82	12.42	1.00	23.52	0.816	37.2804
Case 17	2.82	6.97	2.66	31.16	0.816	35.48369
Case 18	3.87	10.60	1.00	26.46	0.816	25.0057
Case 19	3.87	12.42	1.00	25.95	0.816	21.50924

Table 2 The environmental conditions in L4, wave, wind and current directions in Orcafelx are 180, 157.5 and 135

	Hs (m)	Tp (s)	Gamma	Wind (m/s) 150m	Tidal Current (m/s) on the surface	Occurrences in 11 years (counts/1000)
Case 01	7.844	14.931	1	26.121	0.743	
Case 02	3.569	7.21	3.9	16.7	0.743	
Case 03	4.601	8.727	2.92	19.967	0.743	
Case 04	5.692	10.276	2.22	23.658	0.743	
Case 05	6.885	12.099	1.55	29.764	0.743	
Case 06	6.862	17.73	1	23.05	0.743	
Case 07	5.863	18.59	1	22.155	0.743	
Case 08	4.793	19.419	1	17.184	0.743	
Case 09	1.35	6.67	1.00	22.08	0.743	112.5257
Case 10	1.35	8.68	1.00	22.16	0.743	78.8444
Case 11	1.35	4.67	3.11	22.48	0.743	50.89551
Case 12	2.22	8.68	1.00	23.28	0.743	43.25234
Case 13	2.22	6.67	1.83	31.16	0.743	34.94182
Case 14	1.35	10.68	1.00	20.63	0.743	31.47102
Case 15	2.22	10.68	1.00	24.80	0.743	24.16439
Case 16	3.09	8.68	1.08	30.08	0.743	16.92049
Case 17	3.09	10.68	1.00	26.46	0.743	15.20648
Case 18	1.35	12.69	1.00	18.78	0.743	13.0105
Case 19	1.35	14.69	1.00	17.57	0.743	11.30789

Mooring Configurations for the Two Platforms

The mooring configuration for the full-scale platform consists of three chains, each characterized by uniform properties (shown by Figure 6). This mooring is designed for the deployment at 80 m water depth. The two front moorings primarily resist environmental loads such as wind, waves, and tidal currents, sustaining significant tensile stresses. They employ 105 mm R3 studless mooring chains, each of 550 meters long, deployed symmetrically from the platform's three outer columns at a depth of 14 m below the still water level. The rear chain, measuring 300 meters, experiences comparatively lower loads due to its positioning.

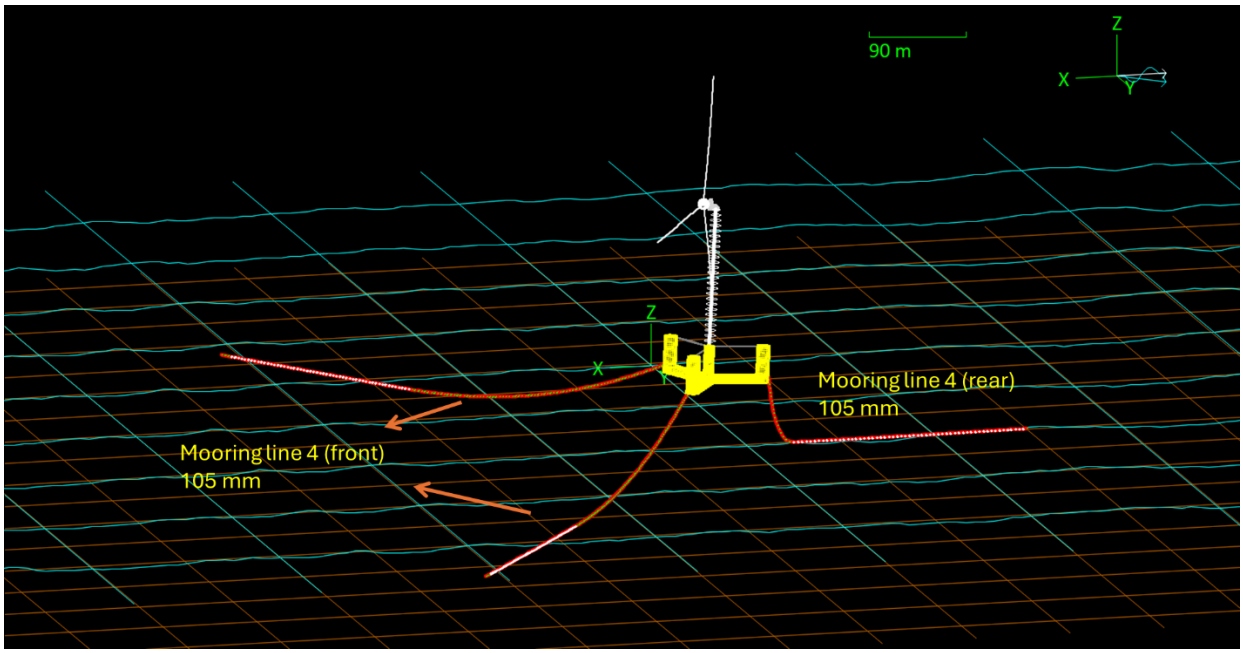

Figure 6 The mooring configuration of the 15MW offshore wind platform

Figure 7shows the mooring configuration of the ACTOR platform, with the test chains as the central components. This mooring is designed for the deployment at 51 m water depth. There are two main test chains (mooring line 1&4) shown in the diagram. The first test mooring line (mooring line 4) is designed to align with the direction of environmental loads, bearing most of these forces. It consists of two sections: the upper section, which connects to the centre bottom of platform, extends 180 m with a bar diameter of 105 mm, while the lower section, connecting the upper part to the seabed, extends 40 m with a bar diameter of 120 mm. The second test mooring line (mooring line 1) is oriented in the opposite direction of the first, connecting to the rear column centre bottom, counterbalancing the system. It extends 220 m with a bar diameter of 105 mm. Another key design objective of the second mooring line is to achieve the required pre-tension, ensuring the system's stability and intended operational conditions. To ensure the platform remains stable and secure, especially in the case of primary test chain failure, the configuration includes two additional safety chains, labelled as Mooring line 3 and 4. These chains follows the same direction as the two front chains of the prototype platform, each extends 300 m with a bar diameter

of 50 mm. These are strategically employed to safeguard the platform, effectively preventing unintended movement or total drift when the test chain is broken during the test. Table 3 lists details of the mooring line system.

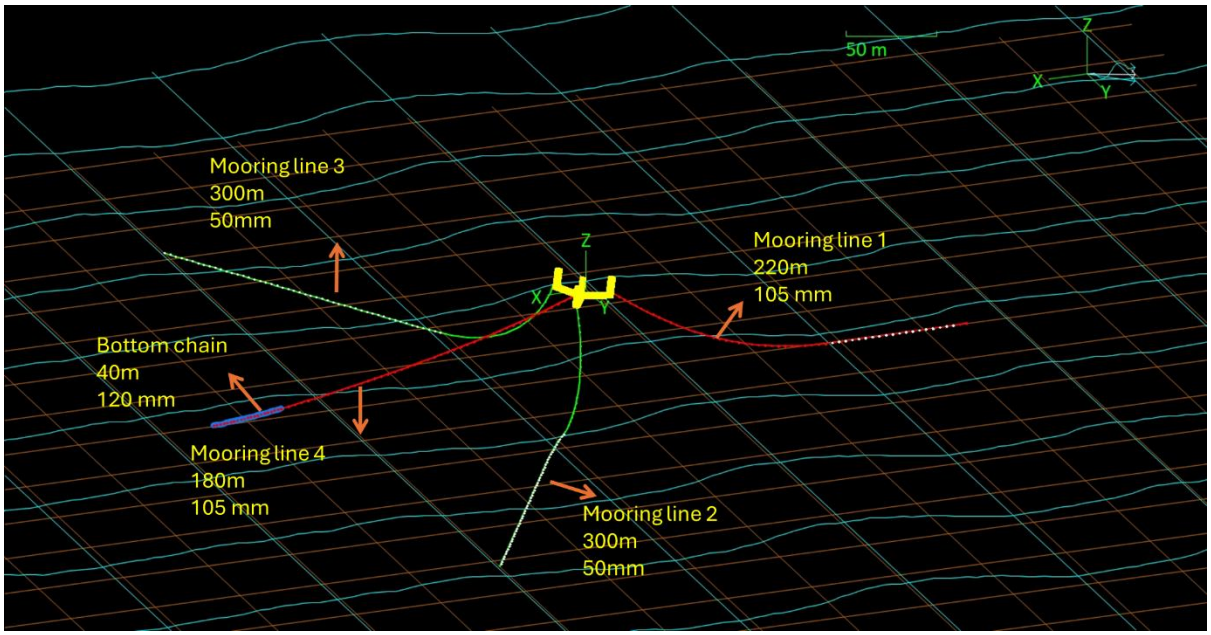

Figure 7 The mooring configuration of the ACTOR platform

Due to the ACTOR platform being situated in a milder sea environment, this mooring system is designed with a suitable level of pre-tension, ensuring that the test chain undergoes equivalent damage cycles and can be fully lifted to replicate peak load conditions observed in the full-scale platform. This ensures that the test chain's loading can encompass the extreme loads experienced in the full-scale platform. Additionally, the test chain can be fully lifted to accelerate fatigue testing. This dual emphasis on performance evaluation and safety highlights the stringent requirements of offshore engineering projects.

Table 3 The key information of the mooring lines

Mooring Line	Bar Diameter (mm)	Link Type	Weight (kN/m)	Pre-tension (kN)	Length (m)
Mooring Line 1 ACTOR	105	Studless	2.15	-	220
Mooring Line 4 ACTOR	105	Studless	2.15	640	180
Mooring Line 2&3 ACTOR	50	Studless	0.49	-	300
Bottom Chain ACTOR	120	Studdenlink	3.09	-	40
Mooring Line 4 Full scaled front	105	Studless	2.15	1644	550
Mooring Line 4 Full scaled front	105	Studless	2.15	1644	300

3. Analyse Approach and Methodology

This study employs time-domain numerical simulations using OrcaFlex (Orcina, 2024) to evaluate mooring system performance for both the full-scale and scaled platforms. Environmental conditions for extreme load and fatigue load have been defined in Table 1 and Table 2. Simulations are performed separately for both platforms, each subjected to environmental loading conditions specific to its proposed deployment site. Mooring configurations are adapted to reflect realistic constraints at each site, while maintaining comparable design intent. The ACTOR platform uses adjusted pre-tension and shallower water depth to induce elevated tension responses. Fatigue damage is estimated using rainflow counting and Miner's rule applied to time-domain tension histories.

By evaluating the frequency and magnitude of extreme loads and fatigue damage, this study assesses whether the ACTOR OffLab platform can serve as a reliable and conservative physical testbed for FOWT mooring system validation.

Extreme load analysis

The extreme load analysis focuses on Cases 01 to 08 for each site, examining the front mooring line tension on the full-scale platform and the test mooring line in the Actor model. The primary objective is to determine whether the ACTOR platform experiences the highest loading or even exceeds the loading conditions observed in the full-scale platform. These eight extreme cases are selected because they correspond to environmental conditions with a 50-year return period, ensuring that the analysis captures the most severe load scenarios that the platform may encounter. By evaluating multiple extreme cases, the study accounts for variations in wave, wind, and current conditions, leading to a more comprehensive understanding of peak loading behaviour.

To systematically analyse extreme loading, the process begins with data filtering, where instances of mooring line tension exceeding a predefined threshold are extracted. The threshold $T_{threshold}$ is defined as:

$$T_{threshold} = \frac{1}{2} T_{max}$$

where T_{max} is the highest recorded tension in the dataset. The filtered tension values are selected as:

$$T_{filtered} = \{T(t) | T(t) \geq T_{threshold}\}$$

After filtering, normalization is applied to scale the tension values relative to the maximum observed tension. The normalized tension $T^*$is given by:

$$T^* = \frac{T_{filtered}}{T_{max}}$$

This normalization ensures that all values fall within the range of 0 to 1, allowing for direct comparison across different cases and environmental conditions.

Once normalized, the data is categorized into bins for statistical evaluation. The binning process segments the tension values into intervals of fixed width ΔT^*,which in this study is set to 0.05. The bin index k for a given tension value $T^*$is calculated as:

$$k = \left\lfloor \frac{T^*}{\Delta T^*} \right\rfloor$$

where $\lfloor \cdot \rfloor$represents the floor function, ensuring that each value is assigned to the appropriate bin.

Finally, density estimation is performed to analyse the distribution of extreme tension values. The probability density function (PDF) $f(T^*)$ is approximated using a kernel density estimation (KDE) method:

$$f(T^*) = \frac{1}{nh} \sum_{i=1}^{n} K\left(\frac{T^* - T_i^*}{h}\right)$$

where $K(\cdot)$is the kernel function, $h$is the bandwidth, and n is the number of data points. This density function provides insight into how frequently different tension levels occur under extreme conditions.

By comparing the density distributions of mooring line tensions from the full-scale platform and the ACTOR platform, the analysis assesses whether the test environment successfully captures the extreme loads expected in real-world conditions. A agreement between these distributions indicates that the scaled testing provides an accurate representation of full-scale extreme loading behaviour, validating the methodology used in the study.

Fatigue analysis

Fatigue analysis in this study is conducted using two computational approaches, both based on rain flow cycle counting to evaluate the cyclic loading characteristics of the mooring system. These methods assess fatigue behaviour by identifying load cycles, computing stress ranges, and estimating cumulative fatigue damage. The ACTOR is a mooring/cable component study. Pre-tension is used to set the mean load and effective stiffness so that the component experiences the appropriate peaks and fatigue cycles in seawater. The intent is not to emulate the complete turbine system but to deliver the correct demand envelope for component qualification

The first method focuses on counting the occurrences of stress cycles, while the second evaluates fatigue damage using a T-N curve and Miner's rule. The analysis begins with data preprocessing, where the tension data is loaded, and a time column is defined. A filtering step is applied to select data within a specific time range to ensure consistency across different simulations. To identify cyclic loading patterns, peak and valley detection is performed. A key filtering criterion is applied, where only peaks and

valleys with a tension difference greater than 1 kN are considered. This threshold is set to remove fluctuations caused by numerical noise and small-scale oscillations that result from simulation errors rather than actual load cycles. While this approach effectively reduces irrelevant fluctuations, it is important to note that setting a fixed threshold, such as 1 kN, might inadvertently exclude low amplitude but genuine fatigue cycles. In cases where smaller stress cycles contribute significantly to fatigue damage accumulation, an adaptive threshold based on a percentage of the mean stress, or a statistical noise model could be a more refined approach. However, for this study, the 1 kN threshold provides a reasonable balance between filtering out numerical noise and retaining meaningful fatigue cycles. Once significant turning points are identified, rainflow cycle counting is applied to quantify stress cycles. This method iterates over the detected turning points, computing stress ranges and mean stresses for each cycle. A stack-based algorithm ensures that each turning point is either paired with a corresponding cycle or temporarily stored for future pairing, accurately modelling the fatigue behaviour of materials under repeated loading.

The second computational approach shifts focus to fatigue damage estimation by incorporating a T-N curve model. The damage calculation follows the standard fatigue damage accumulation approach using Miner's rule:

$$D = \sum_{i=1}^{n} \frac{n_i}{N_i}$$

where D is the cumulative damage, is the number of occurrences of stress cycle i, and $N_i$is the number of cycles to failure for the corresponding stress range, as defined by the T-N curve:

$$N = k\left(\frac{MBL}{\Delta S}\right)^{m}$$

where k and m are empirical fatigue parameters, MBL represents the breaking load of the mooring line, and ΔS the stress range for each identified cycle.

By combining cycle counting and fatigue damage estimation, this methodology provides a comprehensive assessment of the mooring system's fatigue performance. The first approach identifies the frequency of stress cycles, while the second evaluates the severity of damage, ensuring a robust analysis of fatigue life and potential failure points.

Mooring Chain design for ACTOR platform

Based on Table 2, ACTOR platform is expected to experience the most extreme environmental conditions under Case 01. Therefore, the time history results will be used to design the test chain (mooring line 4).

Results from these simulations are depicted in the time histories illustrated in Figure 8 and Figure 9 Back test chain (platform connection point). These figures specifically highlight the maximum tension at the fairlead adjacent to the platform. The maximum tension of the mooring line 4 (3608kN) was recorded at 5920 seconds. Meanwhile, back test chain (mooring line 1) exhibited its maximum tension(2828kN) at 5915 seconds, displaying lower tension characteristics in comparison to the upwind lines.

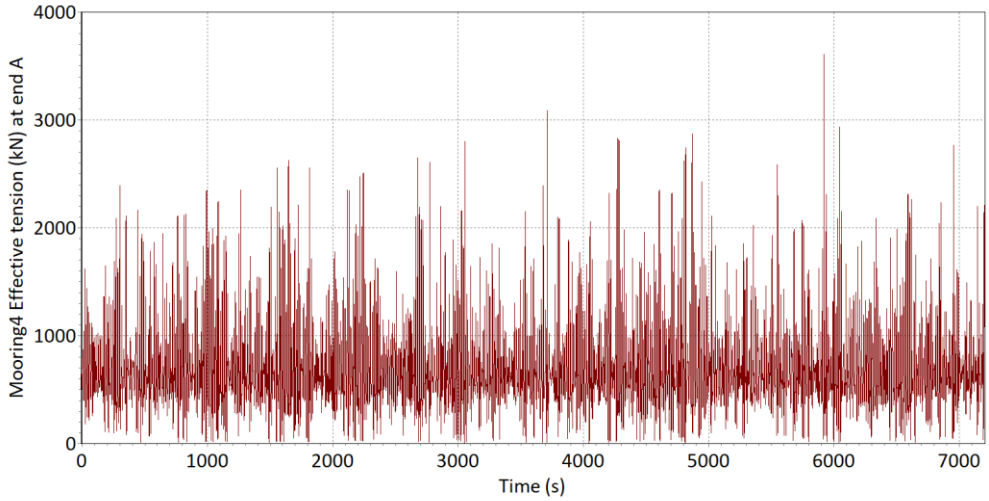

Figure 8 Front test chain (platform connection point)

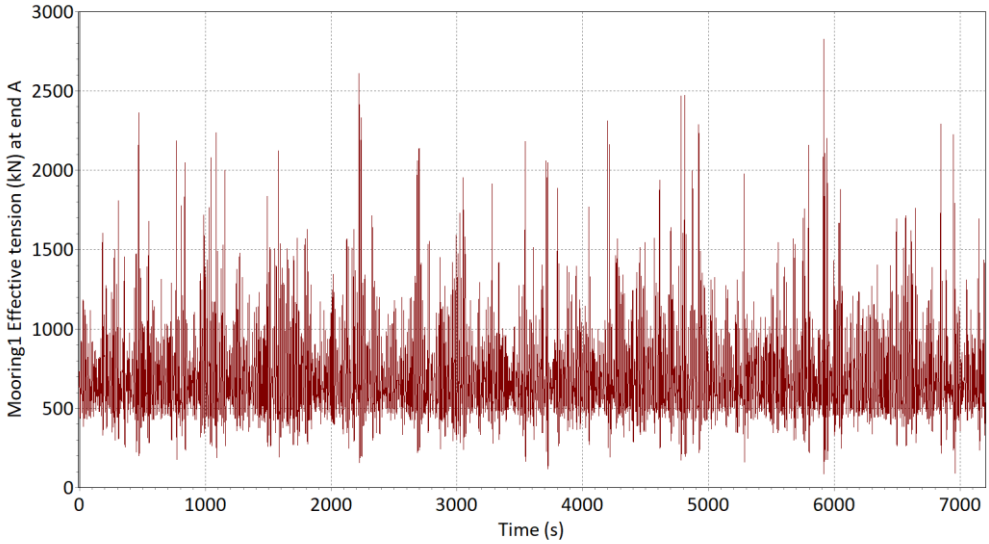

Figure 9 Back test chain (platform connection point)

During the simulations, both test chains were fully lifted, which may have increased fatigue on the mooring lines while accommodating the environmental loading levels typical of a full-scale platform. However, the safety line remained laid on the seabed, even in scenarios where the front test chain was absent. Figure 10 and Figure 11 depict the lift angles of both test chains, where it was noted that the angles of elevation were approximately 10 degrees for each chain. It should be noted that angles of -2

degrees and -178 degrees indicate that an anchor is lying flat along the seabed for the front and back test chains, respectively.

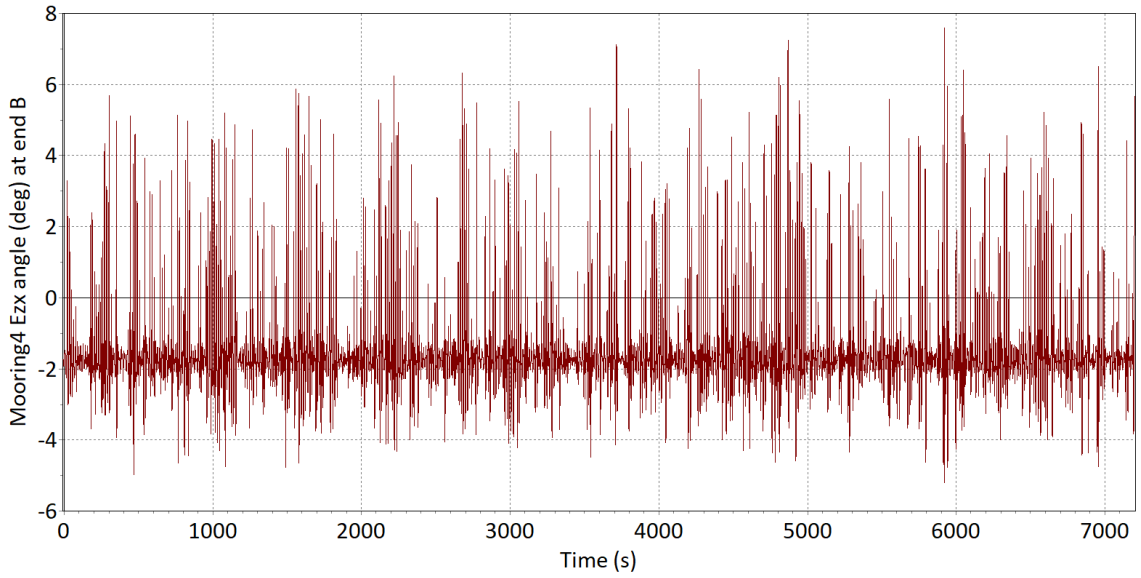

Figure 10 The lifted up degree on the anchor point of front test chain

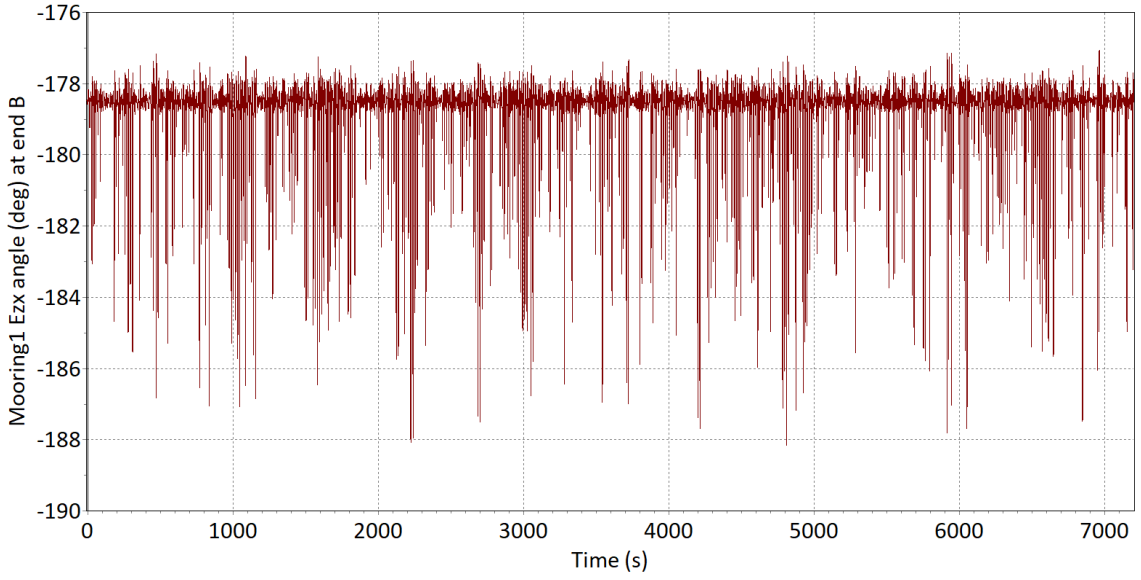

Figure 11 The lifted up degree on the anchor point of back test chain

The mooring design are sourced from industry-standard product catalogues, such as the Sotra Catalogue(Chain, 2021). A key element in the design process involves applying a safety factor (1.67) to the peak tension values derived from simulation data. Consequently, the MBL of each component must surpass this adjusted tension value to ensure reliability and safety. Arrangement and load path from anchor through shackles and chain segments to the instrumented load shackle and fairlead. A parallel safety line provides redundancy and remains slack unless the primary path fails. The

components and their properties for the ACTOR platform mooring chains can be in Figure 12 to Figure 15 and Table 4 to Table 6.

Mooring line 4 (front test line)

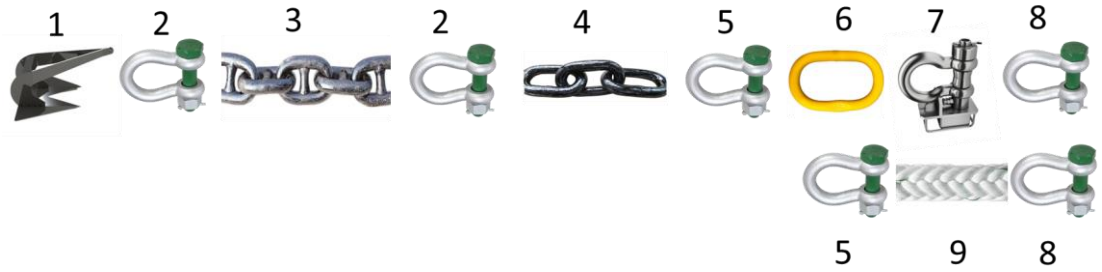

Figure 12 The front test chain components

Table 4 The front test chain components properties

Ref. No	Component name	Properties	Number	Length [m]	Comment
1	Anchor	Further design	1	NA	Pending
2	Bow shackle	WLL 4000 kN	2	NA	Suitable for 120 mm stud link chain
3	Bottom chain	MBL: 11140 kN, Proof loading: 7800kN Grade 3	1	40	120mm diameter needed for weight and test capacity of platform
4	Test chain	MBL: 6123 kN, Proof loading: 8753kN 105 mm Grade 3	1	180	105 mm diameter needed for full scaled platform
5	Bow shackle	WLL 4000 kN	2	NA	Connection of master link , load shackle and the safety line
6	Master link	WLL 4000 kN	1	NA	Connection of load shackle, redundancy line
7	Load shackle	WLL 4000 kN	1	NA	Measurement range based on the expected maximum loads
8	Bow shackle	WLL 4000 kN	2	NA	Connection to the platform to load shackle and safety line
9	Safety line	WLL 7000 kN	1	3	Redundancy line for load shackle

Mooring line 1 (Back test chain)

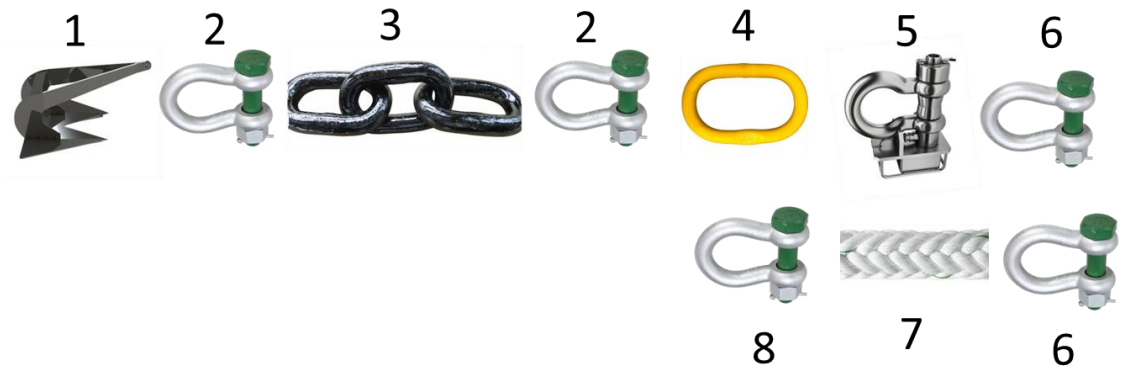

Figure 13 The back test chain components

Table 5 The back test chain components properties

Ref. No	Component name	Properties	Number	Length [m]	Comment
1	Anchor	Further design	1	NA	Pending
2	Bow shackle	WLL 4000 kN	2	NA	Suitable for 105 mm stud less chain
3	Test chain	MBL: 6123 kN, Proof loading: 8753kN 105 mm Grade 3	1	220	105 mm diameter needed for full scaled platform
4	Master link	WLL 4000 kN	1	NA	Connection of load shackle, redundancy line
5	Load shackle	WLL 4000 kN	1	NA	Measurement range based on the expected maximum loads
6	Bow shackle	WLL 4000 kN	2	NA	Connection to the platform to load shackle and safety line
7	Safety line	WLL 7000 kN	1	3	Redundancy line for load shackle
8	Bow shackle	WLL 4000 kN	1	NA	For connection of master link , load shackle and the safety line

Mooring line 2&3 (Safety chains)

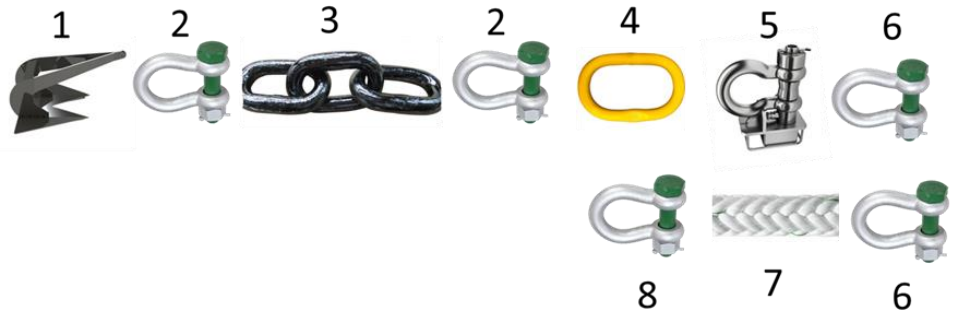

Figure 14 The safety chain components

Table 6 The safety chain components properties

Ref. No	Component name	Properties	Number	Length [m]	Comment
1	Anchor	Further design	1	NA	Pending
2	Bow shackle	WLL 1000 kN	2	NA	Suitable for 50 mm stud less chain
3	small chain	MBL:2230 kN, Proof loading: 1560kN 50 mm Grade 3	1	300	50mm diameter needed for weight
4	Master link	WLL 1000 kN	1	NA	Connection of load shackle, redundancy line
5	Load shackle	WLL 400 kN	1	NA	Measurement range based on the expected maximum loads
6	Bow shackle	WLL 1000 kN	2	NA	Connection to the platform to load shackle and safety line
7	Safety line	WLL 1000 kN	1	3	Redundancy line for load shackle
8	Bow shackle	WLL 1000 kN	1	NA	For connection of master link , load shackle and the safety line

1.

4. Results and Discussions

Extreme load analysis

To assess the extreme loading conditions experienced by the mooring system, a statistical analysis was conducted on the tension distributions observed in the ACTOR platform and the full-scale platform, shown by Table 7 (Skewness and Kurtosis details can be seen in Appendix A). The objective of this analysis was to evaluate whether the scaled model effectively captures extreme tension events and to identify any significant discrepancies that may require further scaling refinements.

To provide a comprehensive assessment of extreme loads, results from Cases 01 to 08 were merged to form a unified dataset for analysis. This approach allows for a more statistically robust comparison between the ACTOR platform and the full-scale platform by incorporating a wide range of extreme loading conditions rather than focusing on isolated cases.

Table 7 The key statistical metrics of the mooring line4 in both ACTOR and Full scaled platform

	ACTOR platform	Full scaled platform
Mean (kN)	667.5551	1331.559
Maximum (kN)	3608.251	3544.378
Skewness	1.724388	0.2195
Kurtosis	6.288981	0.514281

Shown by Table 7, the mean tension in the full-scale platform was found to be significantly higher than in the ACTOR platform, with an average value of 1331.56 kN

compared to 667.56 kN. This difference indicates that the full-scale platform experiences greater sustained loads, due to the hash environmental conditions at Cell22. However, the maximum tension values were similar, with 3608.25 kN recorded for the ACTOR platform and 3544.38 kN in the full-scale platform. The ability of the scaled model to reach peak loading conditions suggests that the pre-tensioning and mooring system adjustments effectively replicate extreme scenarios, even though the average tension remains lower.

While the ACTOR platform successfully reproduces peak loads, its load distribution exhibits significant differences from that of the full-scale platform. The skewness of the tension distribution in the ACTOR platform was calculated as 1.724, considerably higher than the 0.2195 skewness observed in the full-scale platform. The higher skewness in the ACTOR platform suggests that the mooring system in the scaled test is more sensitive to transient high loads, potentially due to localized environmental factors, mooring stiffness differences, or wave energy concentration effects.

Kurtosis further highlights the discrepancy in the frequency of extreme tension events between the two platforms. The ACTOR platform exhibited a kurtosis of 6.289, while the full-scale platform had a kurtosis of 0.514. A high kurtosis value suggests a leptokurtic distribution, meaning that extreme values occur more frequently than in a normal distribution.

To further investigate these differences, a PDF comparison was conducted (see Figure 15). The density distribution of the ACTOR platform exhibited a longer right tail, confirming that extreme high-tension values are more frequent. Conversely, the full-scale platform displayed a more compact and symmetric distribution, indicating that tension values are more evenly spread, with fewer extreme peaks. These findings align with the skewness and kurtosis results.

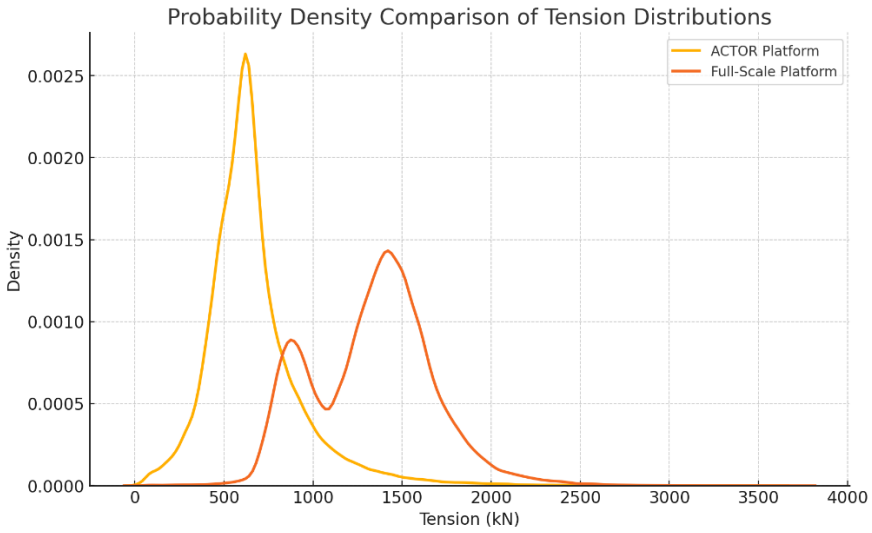

Figure 15 Probability density comparison of tension distributions between the ACTOR platform and the full-scale platform

Fatigue load analysis

The fatigue analysis first focuses on Case 09, which represents the highest occurrence scenario in the dataset. This case serves as a baseline for evaluating fatigue performance between the Full-Scaled platform and the ACTOR methodology, with a primary objective of determining whether ACTOR accelerates fatigue damage accumulation.

The analysis was conducted using tension data analysis, rainflow counting, and damage assessment. Rainflow counting analysis indicated that ACTOR exhibits a higher number of cycles across all stress ranges, with a notable increase in high-stress cycles (>50 kN), as shown in Figure 16. The cycle distribution suggests that ACTOR induces more frequent fatigue loading, leading to accelerated fatigue damage.

As shown in Figure 17, the damage distribution shifts toward higher stress ranges (50-100 kN) in ACTOR, increasing the severity of fatigue loading. The Full-Scaled platform shows damage concentration in the 40-60 kN range, whereas ACTOR extends damage intensity into the 50-100 kN range, confirming that it accelerates fatigue failure. Higher stress ranges contribute significantly to fatigue damage accumulation in ACTOR, leading to reduced fatigue life

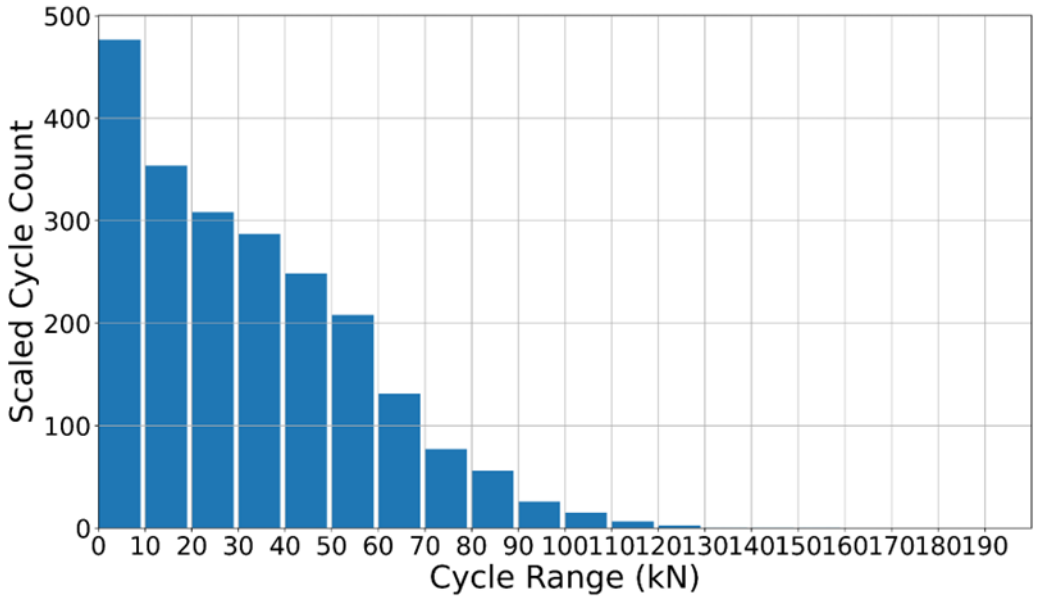

(a)

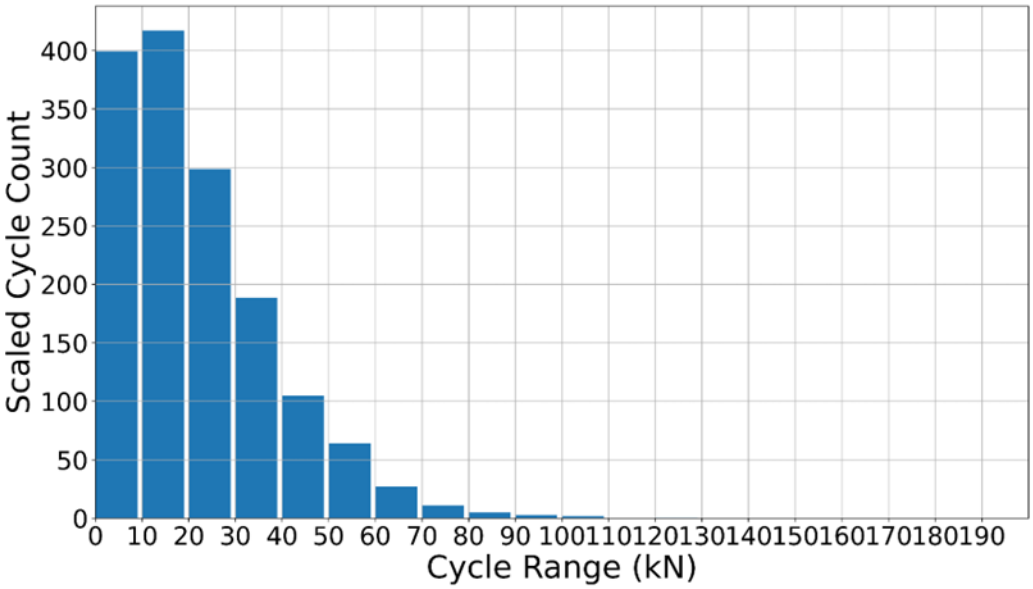

(b)

Figure 16 Rain flow counting in the case 09: (a) ACTOR platform, (b) Full scaled platform

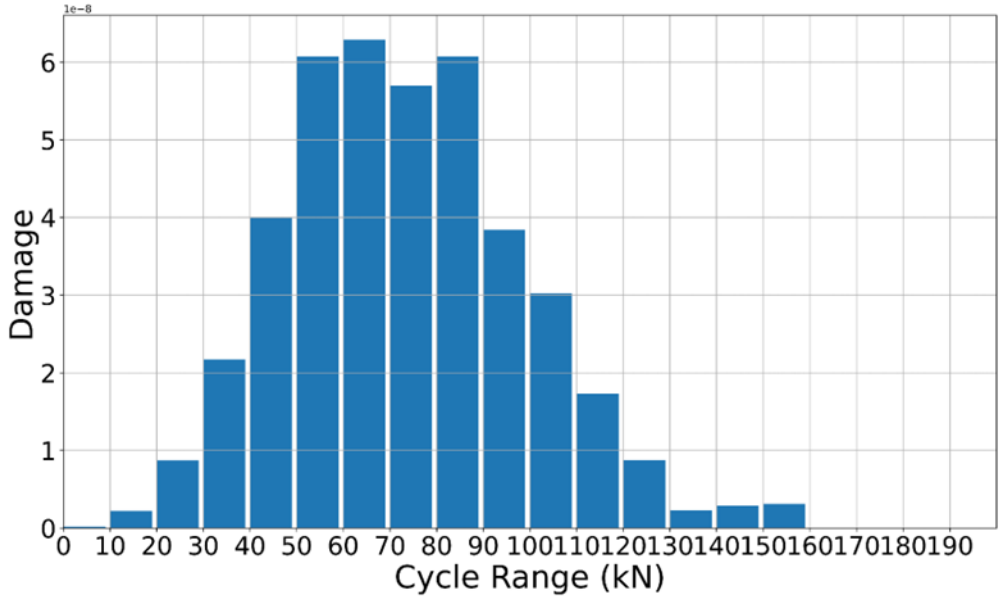

(a)

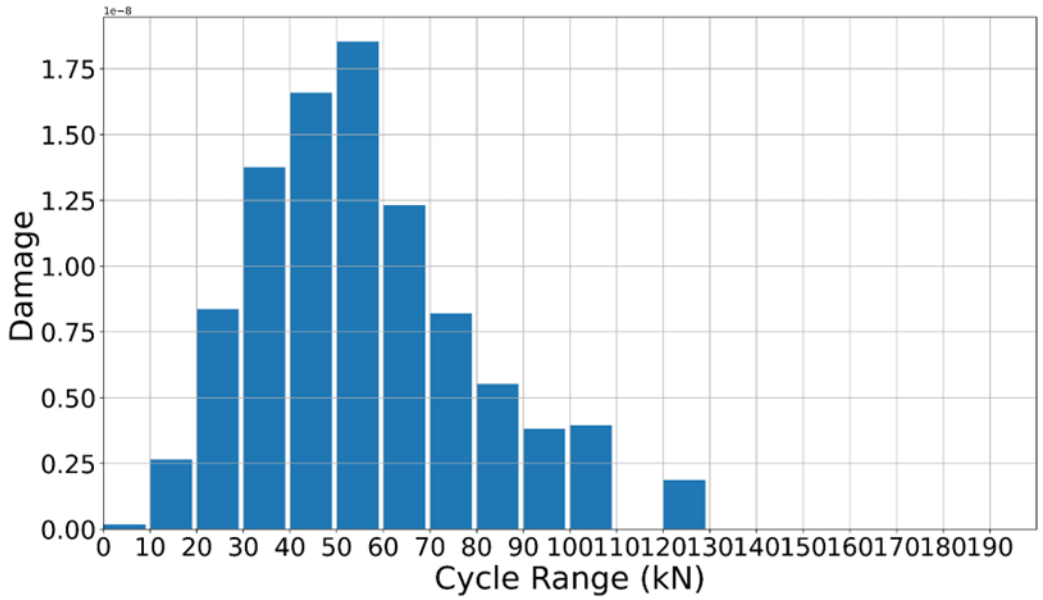

(b)

Figure 17 Rain flow damage in the case 09: (a) ACTOR platform, (b) Full scaled platform

While Case 09 provides critical insight into fatigue performance, real-world fatigue behaviour cannot be fully captured through a single-case study. Therefore, the analysis is extended to Case 09-19, incorporating multiple scenarios with varying exposure times to better understand long-term fatigue trends.

The total exposure time for Case 09-19 over 11 years is 96,360 hours, with Full-Scaled cases accounting for 54,392 hours and ACTOR accounting for 41,632 hours, see Table 8. Although ACTOR has a lower total exposure time, its fatigue impact remains disproportionately high due to an increased cycle count and higher stress concentrations.

Table 8 The exposure time of case 09-19

	Full Scaled (hours)	ACTOR (hours)
Case 09	9572.79	10842.97
Case 10	7273.71	7597.446
Case 11	7150.05	4904.291
Case 12	5271.43	4167.795
Case 13	5021.36	3366.994
Case 14	4385.72	3032.548
Case 15	4223.85	2328.48
Case 16	3592.33	1630.458
Case 17	3419.20	1465.296
Case 18	2409.55	1253.691
Case 79	2072.63	1089.629
Total (case 09-19)	54392 (54.3%)	41632 (42%)
Total 11years hours	96360	96360

Rainflow counting analysis for Case 09-19 (see Figure 18)shows that ACTOR continues to exhibit a higher number of stress cycles across all ranges, with a notable increase in cycles above 50 kN. Compared to Case 09 alone, the broader dataset reveals a more comprehensive trend, confirming that ACTOR systematically increases fatigue loading across multiple cases.

The total fatigue damage comparison further validates this trend (see Figure 19). While Case 09 primarily shows peak damage accumulation between 50-70 kN, the merged analysis for Case 09-19 demonstrates a shift towards higher stress ranges (50-190 kN), intensifying fatigue severity. ACTOR's fatigue damage continues to increase at higher stress levels, whereas Full-Scaled damage remains concentrated in mid-range stresses.

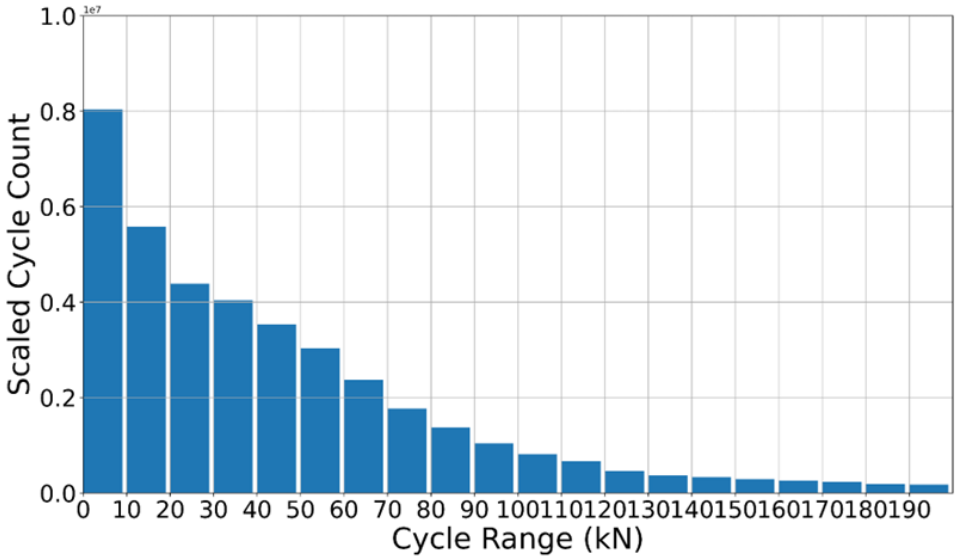

(a)

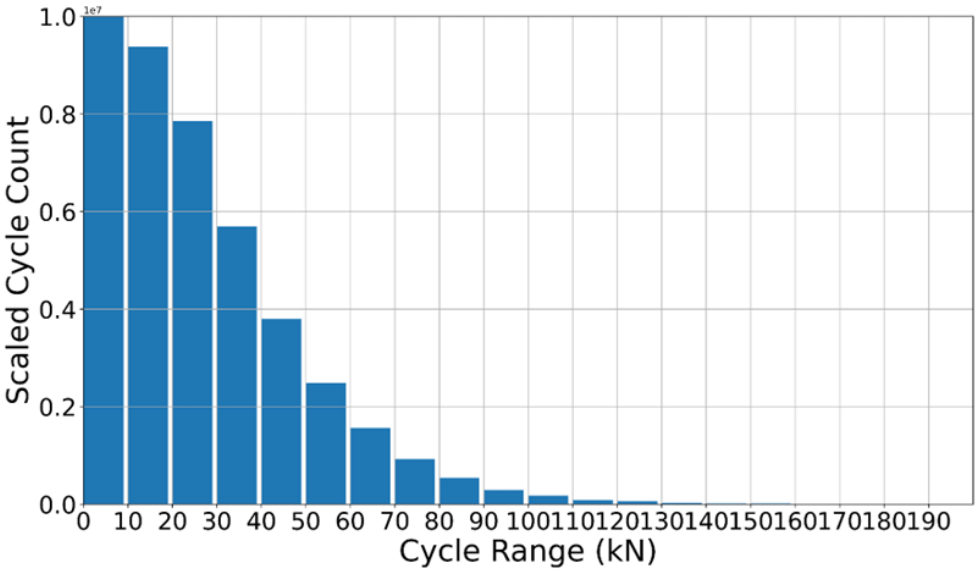

(b)

Figure 18 Rain flow counting in the case 09-19: (a) ACTOR platform, (b) Full scaled platform

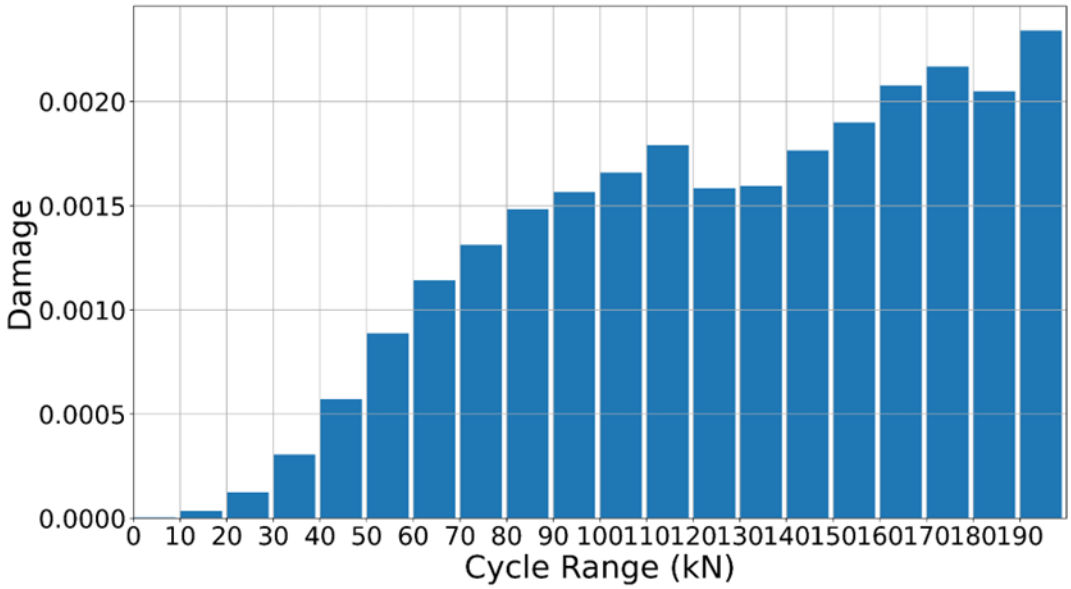

(a)

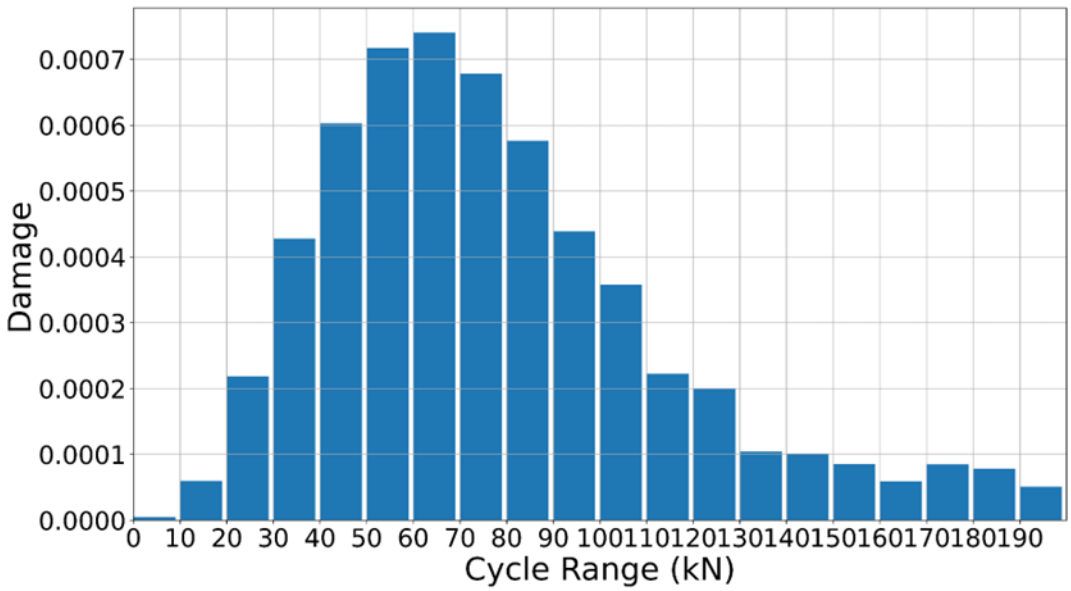

(b)

Figure 19 Rain flow damage in the case 09-19: (a) ACTOR platform, (b) Full scaled platform

Further extending the analysis, the fatigue life of mooring lines under both Full-Scaled and ACTOR conditions was evaluated. As shown in Figure 20, the full-scale platform exhibits a significantly longer mooring chain life than the ACTOR platform. In the full-scale platform, some portions of the mooring chain remain in contact with the seabed, which influences its fatigue performance in two keyways. First, seabed contact helps redistribute the load, allowing a portion of the mooring line tension to be absorbed by the seabed rather than fully transmitted to the floating platform. This reduces dynamic stress variations in the upper sections of the mooring chain. Second, friction between the mooring chain and the seabed provides a natural damping effect, which dissipates energy from environmental forces and limits the frequency and amplitude of cyclic loading. Because of these combined effects, the full-scale mooring system experiences lower stress fluctuations, leading to fewer high-stress fatigue cycles and an estimated mooring line lifespan of approximately 63 years.

In contrast, the ACTOR platform allows the test mooring chains remain fully lifted from the seabed during testing. This intentional design choice was made to replicate extreme load conditions and accelerate fatigue accumulation within a controlled testing period. The absence of seabed contacts results in increased dynamic loading, as the mooring chains are fully exposed to wave and current-induced cyclic stresses. Additionally, because the chains are completely suspended, they experience higher stress ranges without the seabed's natural damping effect. This leads to frequent and high-amplitude load variations, significantly accelerating fatigue damage accumulation.

The rainflow cycle counting analysis again confirms that ACTOR experiences approximate 5.5 times higher fatigue damage accumulation compared to the full-scale

platform. As a result, the expected fatigue life of the mooring system is drastically reduced from 63 years in the full-scale platform to approximately 11.6 years in the ACTOR platform. The findings demonstrate that while the ACTOR platform successfully replicates peak mooring loads, its accelerated fatigue behaviour provides valuable insights into long-term mooring performance, contributing to more efficient and cost-effective offshore wind technology validation.

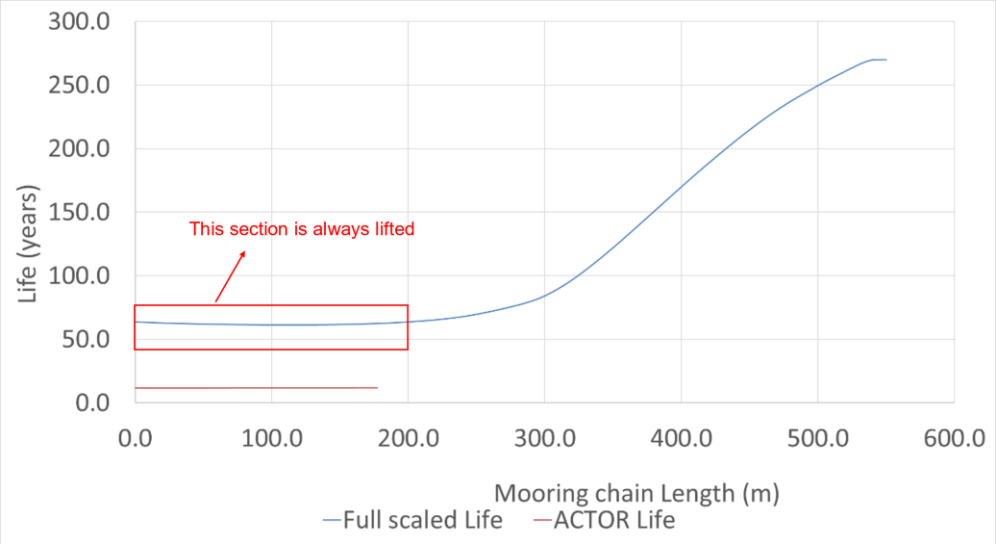

Figure 20 The mooring line life in both ACTOR and Full scaled platform

ACTOR application

This study frames ACTOR as a component-test platform rather than a geometrically scaled turbine model. The criterion for representativeness is that the platform must (i) reproduce the full-scale peak line tension within a narrow band and with the same safety factor used for design checks and (ii) accelerate fatigue in a controlled manner to compress test duration. In the present case ACTOR reached 3608 kN versus 3544 kN at full scale and showed a markedly shorter life due to full lift and higher effective stiffness in 51 m water depth, which is intentional for accelerated mooring qualification. Unlike a purely analytical increase of safety factor, accelerated testing at ACTOR subjects full-size mooring components to real seawater cycles, capturing wear, corrosion-fatigue interaction, and load-path nonlinearities.

Before testing, simulations are used to set the ACTOR pre-tension so that the mooring line on ACTOR reaches the same maximum line tension as expected in the reference full-scale platform. The measured tension time series during ACTOR deployment then confirms whether the actual hardware survives this ultimate load under the prescribed design safety factor. This provides direct evidence that the full-size component can withstand the peak demand it would experience offshore.

By adjusting pre-tension, ACTOR also produces more frequent chain lift and higher stress ranges, which accelerates fatigue damage compared to the offshore case.

Damage rates derived from ACTOR tension histories (via rain flow counting and Miner's rule) can therefore be converted into equivalent full-scale operating hours. This allows a shorter test campaign to provide meaningful information on long-term durability of the component.

The same procedure can be applied to different mooring or cable designs, including new materials. By setting pre-tension to reach the full-scale peak and by measuring fatigue under accelerated conditions, ACTOR provides a conservative and efficient way to qualify new components before offshore deployment.

In the present case ACTOR reproduced the offshore peak (3608 kN vs 3544 kN) and delivered a $\approx 5.5\times$ higher fatigue rate, so months of ACTOR exposure correspond to many months of offshore operation. These data directly inform full-scale design by confirming ultimate strength, by quantifying fatigue endurance in seawater, and by providing a practical framework for testing novel mooring and cable technologies under accelerated but conservative conditions.

5. Conclusions

This study presented a comparative mooring analysis between a full-scale 15 MW floating wind turbine and a 1:3 scaled conceptual offshore laboratory platform (ACTOR), aimed at assessing its suitability as a conservative testbed for mooring system evaluation. The findings indicate that, despite being deployed in a nearshore site with milder environmental forcing, the ACTOR platform can replicate or exceed mooring tensions and fatigue accumulation observed in deeper offshore environments due to its shallow water depth and optimized pre-tension configuration. The main findings are summarized as follows:

- Extreme Load Validation: The extreme load analysis confirmed that, while the ACTOR platform operates in a reduced environmental force regime, The implementation of a suitable pre-tension level ensures that peak tension conditions are replicated while simultaneously accelerating fatigue damage accumulation. The peak mooring line tensions recorded were 3608 kN for the ACTOR platform and 3544 kN for the full-scale platform, indicating that the ACTOR system can effectively mimic full-scale extreme loading conditions. However, statistical analysis revealed differences in load distribution, with ACTOR exhibiting higher skewness (1.724) and kurtosis (6.289), suggesting more frequent transient extreme loads due to differences in environments and pre-tension.

- Fatigue Acceleration: The ACTOR platform significantly accelerates fatigue damage accumulation compared to the full-scale model. Rainflow cycle counting analysis showed that the ACTOR platform experienced round 5.5 times more fatigue damage, primarily due to the increased number of high-

stress cycles exceeding 50 kN. The fatigue life estimation demonstrated a substantial reduction from 63 years (full-scale) to 11.6 years (ACTOR), confirming its ability to accelerate the assessment of long-term mooring durability within a compressed timeframe.

- Mooring Test Chain Design: Based on the Orcaflex simulations and industry information, a specialized test chain was designed for the ACTOR platform. The mooring chain components were selected based on simulated peak tension values with a safety factor of 1.67, ensuring structural integrity under testing conditions.

These results reinforce ACTOR's conceptual role as a bridge between numerical modeling and full-scale deployment. As a future step, physical construction and instrumentation of ACTOR will enable real-world validation of simulation results and further calibration of mooring response models. Once deployed, ACTOR will support accelerated life testing, sensor validation, and digital twin development for offshore renewable energy systems. Its accessibility, lower operational cost, and data-rich environment make it a valuable resource for de-risking offshore components and advancing floating wind technology readiness.

Future research will focus on improving environmental scaling methodologies, particularly in pre-tension adjustments, to further refine load distribution accuracy. Additionally, integrating real-time monitoring through digital twin technologies and expanding full-scale validation campaigns will strengthen the applicability of ACTOR findings to real offshore wind farms, ensuring more reliable and scalable offshore energy solutions.

Acknowledgements

We like to acknowledge the support through Innovate UK towards the WEDUSEA project [10103051] which sponsors the first author; support through EPSRC towards the ORE Supergen Hub [EP/S000747/1] which sponsored the second author; as well as support through the CIoS Good Growth fund towards the COMAC [BUS003_0112] project and the University of Plymouth that provided support through the OcEn project.

References

Allen, C., Viscelli, A., Dagher, H., Goupee, A., Gaertner, E., Abbas, N., Hall, M., & Barter, G. (2020). *Definition of the UMaine VolturnUS-S reference platform developed for the IEA wind 15-megawatt offshore reference wind turbine*.

Carpintero Moreno, E., Stratigaki, V., Troch, P., De Pauw, B., & Baur, T. (2020). Blue Accelerator: the new testing site in Ostend for maritime technology developments to enhance Blue Economy. General Assembly,

Chain, S. A. a. (2021). *Anchor and Chain Handbook 8th Edition*. https://www.sotra.net/contact/order-handbook/

Clark, D. S. B. A. J. B. R. (2024). *RISK ENGINEERING GUIDELINES FOR THE INSURANCE OF FLOATING OFFSHORE WIND FARMS* https://www.iua.co.uk/IUA_Member/Clauses/eLibrary/Clauses_Summary.aspx?DocumentKey=B508F167-C965-4707-9CE8-67EE124698ED

Dobson, T., Lenchine, V., & Bainbridge, S. (2024). A review on the interactions between engineering and marine life: key information for engineering professionals. *Journal of Ocean Engineering and Marine Energy*, *10*(2), 449-459.

Estate, T. C. (2023). *The Crown Estate refines plans for Celtic Sea floating wind | 2023—The Crown Estate refines plans for Celtic Sea floating wind*. https://www.thecrownestate.co.uk/en-gb/media-and-insights/news/2023-the-crown-estate-refines-plans-for-celtic-sea-floating-wind/

Gaertner, E., Rinker, J., Sethuraman, L., Zahle, F., Anderson, B., Barter, G., Abbas, N., Meng, F., Bortolotti, P., & Skrzypinski, W. (2020). Definition of the IEA 15-megawatt offshore reference wind turbine.

Graham, J. A., O'Dea, E., Holt, J., Polton, J., Hewitt, H. T., Furner, R., Guihou, K., Brereton, A., Arnold, A., & Wakelin, S. (2018). AMM15: a new high-resolution NEMO configuration for operational simulation of the European north-west shelf. *Geoscientific Model Development*, *11*(2), 681-696.

Hersbach, H., Bell, B., Berrisford, P., Hirahara, S., Horányi, A., Muñoz-Sabater, J., Nicolas, J., Peubey, C., Radu, R., & Schepers, D. (2020). The ERA5 global reanalysis, quarterly journal of the royal meteorological society.

Hmedi, M., Uzunoglu, E., Zeng, C., Gaspar, J., & Guedes Soares, C. (2023). Experimental challenges and modelling approaches of floating wind turbines. *Journal of Marine Science and Engineering*, *11*(11), 2048.

Mackay, E., & de Hauteclocque, G. (2023). Model-free environmental contours in higher dimensions. *Ocean Engineering*, *273*, 113959.

Matha, D., Schlipf, M., Pereira, R., & Jonkman, J. (2011). Challenges in simulation of aerodynamics, hydrodynamics, and mooring-line dynamics of floating offshore wind turbines. ISOPE International Ocean and Polar Engineering Conference,

Mazzaretto, O. M., Menéndez, M., & Lobeto, H. (2022). A global evaluation of the JONSWAP spectra suitability on coastal areas. *Ocean Engineering*, *266*, 112756.

McCoy, A., Musial, W., Hammond, R., Mulas Hernando, D., Duffy, P., Beiter, P., Perez, P., Baranowski, R., Reber, G., & Spitsen, P. (2024). *Offshore Wind Market Report: 2024 Edition*.

Orcina. (2023). *Comparison of loads from OrcaFlex and OpenFAST for the IEA 15 MW RWT*. https://www.orcina.com/wp-content/uploads/resources/validation/R15120101-OrcaFlex-15MW-RWT-Validation-Report.pdf

Shimada, S., Kogaki, T., Konagaya, M., Mito, T., Araki, R., Ueda, Y., & Ohsawa, T. (2022). Validation of near‐shore wind measurements using a dual scanning light detection and ranging system. *Wind Energy*, *25*(9), 1555-1572.

Timmington, D., & Efthimiou, L. (2022). Mooring Systems for Floating Offshore Wind: Integrity Management Concepts, Risks and Mitigation. World Forum Offshore Wind,

Touzon, I., Nava, V., Gao, Z., Mendikoa, I., & Petuya, V. (2020). Small scale experimental validation of a numerical model of the HarshLab2. 0 floating

platform coupled with a non-linear lumped mass catenary mooring system. *Ocean Engineering*, *200*, 107036.

Tumse, S., Bilgili, M., Yildirim, A., & Sahin, B. (2024). Comparative Analysis of Global Onshore and Offshore Wind Energy Characteristics and Potentials. *Sustainability*, *16*(15), 6614.

Yang, R., Zheng, X., Chen, J., & Wu, Y. (2022). Current status and future trends for mooring systems of floating offshore wind turbines. *Sustainable Marine Structures*, *4*(2), 40-54.

Appendix A. Skewness and Kurtosis

A.1 Physical meaning

- **Skewness** describes whether the data distribution is symmetric or biased to one side.
  - Positive skewness → more frequent or larger **high-tension peaks**.
  - Negative skewness → more frequent or larger **low-tension dips**.
- **Kurtosis** describes how "heavy" the tails are compared to a normal distribution.
  - High kurtosis → more extreme values (rare but very high or very low tensions).
  - Low kurtosis → fewer extremes, values clustered closer to the mean.

A.2 Equations

Skewness

$$g_1 = \frac{n}{(n-1)(n-2)} \sum_{i=1}^{n} \left(\frac{x_i - \bar{x}}{s}\right)^3$$

Excess Kurtosis

$$g_2 = \frac{n(n+1)}{(n-1)(n-2)(n-3)} \sum_{i=1}^{n} \left(\frac{x_i - \bar{x}}{s}\right)^4 - \frac{3(n-1)^2}{(n-2)(n-3)}$$

Where:

- x_i is each sample (e.g., mooring line tension at time step iii)
- $\bar{x}$ is sample mean
- s is sample standard deviation
- n is number of samples

A.3 Relevance for this paper

In this study, skewness and kurtosis are used to compare the **statistical shape** of mooring line tension time histories between the **full-scale platform** and the **ACTOR platform**.